國立臺灣大學醫學院分子醫學所

碩士論文

Institute of Molecular Medicine

College of Medicine

National Taiwan University

Master's Thesis

成體神經幹細胞衰老過程中蛋白質恆定之角色探討

Investigation of proteostasis in adult neural stem cell aging

黃蔓鈞

Man-Chun Huang

指導教授：阮麗蓉 博士

Advisor: Dr. Li-Jung Juan

中華民國 113 年 2 月

February 2024

國立臺灣大學碩士學位論文
口試委員會審定書
MASTER'S THESIS ACCEPTANCE CERTIFICATE
NATIONAL TAIWAN UNIVERSITY

成體神經幹細胞衰老過程中蛋白質恆定之角色探討

Investigation of proteostasis in adult neural stem cell aging

本論文係黃蔓鈞（R10448004）在國立臺灣大學分子醫學研究所完成之碩士學位論文，於民國 112 年 12 月 15 日承下列考試委員審查通過及口試及格，特此證明。

The undersigned, appointed by the Graduate Institute of Molecular Medicine on 15 December 2023 have examined a Master's Thesis entitled above presented by Man-Chun Huang (R10448004) candidate and hereby certify that it is worthy of acceptance.
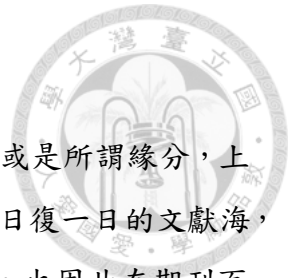
口試委員 Oral examination committee:

（指導教授 Advisor）

系（所、學位學程）主管 Director:

序言/謝詞

外婆失智帶來的煩惱，已在兩年來漸漸習慣，不知是巧合，或是所謂緣分，上天賦予了我研究老化最好的意義和註解。面對不斷失敗的實驗、日復一日的文獻海，埋首微觀世界裡的同時我的外婆卻以光速在宏觀的世界裡老去。也因此在期刊百家爭鳴與點數爭取如此不易的年代，我得以心安理得的為研究生物的初衷負責，感謝得來不易的機會使我能投身老化領域，這是我的幸運，也是對自我的期許。

這篇研究的進行，首先必須感謝阮麗蓉老師。跟隨老師不知不覺已過三個年頭，還記得第一次參加研討會，就因老師的認真而震驚，我想每個人追隨一位老師一定有原因，而對我來說那就是老師熱衷學術閃閃發亮的樣子。我很感謝老師在我新冠肺炎確診時說要寄清冠一號給我，也很感謝老師花了數小時與我討論未來，並一路給我鼓勵。如同老師所說，實驗室的成員們一榮俱榮，若非實驗室的經費、時間支持，不可能有這篇研究的誕生。

提到實驗室成員，我最想感謝的是我的共同研究伙伴，也是我的好前輩、好朋友，林文淵博士。謝謝你和我一起渡過焦慮、苦惱、疲倦、失落，也謝謝你與我分享喜悅、興奮、感動、和歡笑。你總是讓事情變得充滿希望和有趣，讓我對做研究有不一樣的看法，我知道伯樂難遇，知音難尋，而因為你我兩者兼得。我也想感謝郭承鑫博士阿鑫，有你在的時候就有笑聲，雖然因為你不喜歡學長學弟制才有了阿鑫這個稱號，但你從不吝於教我實驗、分享經驗，也很嚴謹認真的面對每一個成果，在我心中你絕對是個很罩的學長和朋友。感謝明倫、秀芬提供我非常多協助，謝謝基因體中心的核心設施質譜儀實驗室的建弘和流式細胞儀實驗室的文文在實驗上提供專業意見，也謝謝中研院統計合作社跟我們討論統計方式。

最後謝謝我的爸爸媽媽和乾爹，我最愛的家人們，很抱歉我常常晚回家或是在忙，從永和到中研院真的很遠，但很多時候媽媽還是不嫌麻煩的載我去，滿桌熱呼呼的菜更是我回家的動力，如同二十多年來的日復一日，你們從來不假思索的給我支持，唸生物不是一條風平浪靜的康莊大道，但你們相信我的每一個選擇，並讓我無後顧之憂的前進。謝謝我的男朋友李岳陽當我最強大的後盾，無論發生甚麼都有你在身旁，你總是在假日陪我加班，或晚上突然出現給我驚喜，帶著我最喜歡的點心，謝謝你給我滿滿的愛跟無微不至的照顧，帶我去任何我想去的地方、陪我做任

ii

何我想做的事，讓我在24歲還能無憂無慮的做夢。謝謝我的朋友們，聽我分享研究生活中的各種大小事，陪我一起擔心開心。謝謝身邊愛我和我愛的每一個人，因為你們我是如此幸福。

最後的最後，感謝因為這篇研究而犧牲的老鼠，你們並非只是許多研究者口中的一團會動的蛋白質，也不是只出現在材料與方法的幾行字，我知道自己有許多不足，也因為這些不足讓你們受了許多苦，謝謝你們令我思考，時時刻刻提醒我科學面對的是活生生的生命，希望你們離去時沒有苦痛和恐懼，並希望仍活著的生命都能被溫柔且善良的對待與珍惜。

中文摘要

　　成體神經幹細胞（neural stem cells, NSCs）的衰退與認知功能障礙和老化相關的神經退化性疾病有關。最近的研究顯示在成年哺乳動物的大腦中，主要有再生能力的成體神經幹細胞位於側腦室的腦室下區（subventricular zone, SVZ）以及海馬迴的齒狀回（dentate gyrus, DG）。隨著老化的進程，蛋白質體平衡（proteostasis）的失衡增加了異常蛋白聚集的風險，同時也是老化和許多神經退行性疾病的標誌。儘管目前有關於中年老鼠（12 個月大）和年輕成年 NSCs（2 個月大）蛋白質體的研究，但尚未有專門針對高齡老鼠（20-21 個月大）和年輕老鼠（2 個月大）進行得比較。

　　在與博士後研究員林文淵博士的合作下，我們對 21 種不同的 NSC 培養基進行了神經球（neurosphere）形成效能測試。其中包括 8 種先前已發表的培養基和 13 種由三種基礎培養基和兩種常用於神經細胞培養的添加物組合而成的培養基。我們發現其中一種先前被用於將幹細胞分化為神經細胞的培養基（M12），展現了最佳的神經球形成能力。在相同的條件下，它形成了最多且最大的神經球，揭示了其在神經球培養中的重要性和應用性。此外，在 13 種未被發表過的培養基中，我們的結果顯示其中 3 種具有形成神經球的能力。在本研究中，我們使用 M12 培養由年輕和高齡小鼠 SVZ 細胞形成的神經球做為研究模型。

　　關於老年老鼠的 SVZ 細胞形成神經球的能力是否下降一直存在爭議，因此我們比較了老年和年輕老鼠的 SVZ 細胞形成神經球的能力。我們的結果支持 SVZ 細胞形成神經球的能力隨年齡下降的論點，顯示老年老鼠的 SVZ 細胞形成的神經球明顯較年輕的少，並且其增殖能力也顯著降低。此外，與先前的研究一致，經過兩次繼代後，這種老年神經球形成能力下降的特性不復存在。我們的培養系統保留了老年神經幹細胞增殖能力降低的特性，這也與已知的大腦內成年神經新生（neurogenesis）在老化過程中下降的情況一致。

　　鑒於蛋白質 N 端乙醯化（N-terminal acetylation，NAc）在老化期間對蛋白質體平衡的重要性，我們還分析了年輕和老年神經球內蛋白質 N 端乙醯化比例的變化。使用高鹼性逆相層析分離（High pH reversed-phase liquid chromatography, RPLC）搭配液相層析串聯式質譜儀（LC-MS/MS），我們識別出 N 端乙醯化程度受年齡調

控的蛋白。其中，TMSB10（Thymosin beta-10）、PPIA（Peptidyl-prolyl cis-trans isomerase A）、SLC6A11（Sodium- and chloride-dependent GABA transporter 3）和 PSMD1（26S proteasome non-ATPase regulatory subunit1）的 N 端乙醯化程度在高齡神經球中顯著提高，而 DDT（D-dopachrome decarboxylase）則顯著降低。此外我們發現老年神經球中未修飾的蛋白質 N 端程度降低，暗示其蛋白質 N 端乙醯化提高的可能，且未修飾的蛋白質 N 端程度在 SVZ 和 DG 中呈現組織特異性。這些發現提供了成年神經幹細胞老化的潛在調節機制，並有助於更深入探討成體神經幹細胞老化的原因。
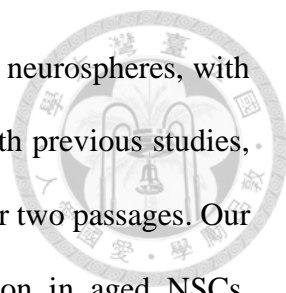
關鍵字: 神經幹細胞、腦室下區、神經球、蛋白質體、N 端乙醯化

Abstract
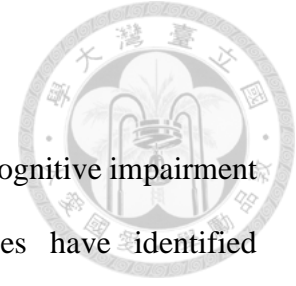
The decline of adult neural stem cell (NSC) has been linked to cognitive impairment and aging-associated neurodegenerative diseases. Recent studies have identified regenerative-capable NSCs in the adult mammalian brain primarily localized within the subventricular zone (SVZ) of the lateral ventricle and the dentate gyrus (DG) of the hippocampus. During aging, the loss of proteostasis increases the risk of abnormal protein aggregates, marking a hallmark of aging and many neurodegenerative diseases. Despite current studies on the proteome of middle-aged mice (12 mo.) and young adult NSCs (2 mo.), there has been no comparison specifically for aged mice (20-21 mo.) and young mice (2 mo.).

In collaboration with postdoc Wen-Yuan Lin, we conducted neurosphere-forming efficiency tests on 21 different NSC culture media. These included 8 media previously published and 13 media formulated by combining three basal mediums and two supplements commonly used for neural cell culture. We found that one of the culture media (M12), previously used for differentiating stem cells into neural cells, exhibited the best neurosphere-forming ability. Under the same conditions, it formed the most and largest neurospheres, revealing its importance and applicability in neurosphere culture. Additionally, among the 13 unpublished culture media, we identified three with neurosphere-forming capabilities. Therefore, we used M12 culture medium to cultivate neurospheres formed by young and aged mouse SVZ cells as our research model.

Due to controversies in previous research regarding whether the neurosphere-forming ability of SVZ cells in aged mice declines, we initially compared the neurosphere-forming capabilities of SVZ cells from aged and young mice. Supporting the viewpoint that the neurosphere-forming ability of SVZ cells decreases with age, our

results showed that SVZ cells from aged mice notably formed fewer neurospheres, with their proliferation capacity decreased. Furthermore, in alignment with previous studies, the age-dependent decline in neurosphere-forming ability ceased after two passages. Our culture system retained the characteristic of decreased proliferation in aged NSCs, consistent with the known in vivo decline in adult neurogenesis with aging.

Additionally, owing to the importance of protein N-terminal acetylation (NAc) in proteostasis during aging, we also analyzed the change in protein N-terminal acetylation ratio within young and old neurospheres. We conducted a comprehensive analysis using high pH reversed-phase liquid chromatography (RPLC) coupled with LC-MS/MS. The proteomic analysis identified proteins with a change in the N-terminal acetylation ratio associated with age. In the aged neurospheres, the N-terminal acetylation levels of TMSB10 (Thymosin beta-10), PPIA (Peptidyl-prolyl cis-trans isomerase A), SLC6A11 (Sodium- and chloride-dependent GABA transporter 3), and PSMD1 (26S proteasome non-ATPase regulatory subunit1) were significantly increased, while DDT (D-dopachrome decarboxylase) exhibited a significant decrease. Besides, our study unveiled elevated levels of N-terminal acetylation in aged neurospheres, displaying tissue-specific patterns in DG and SVZ. These findings provide potential regulatory mechanisms underlying the aging process of adult NSCs and contribute to a deeper understanding of the reasons behind it.
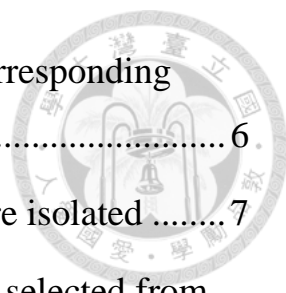
Keywords: Neural stem cells, subventricular zone, neurospheres, proteostasis, N-terminal acetylation
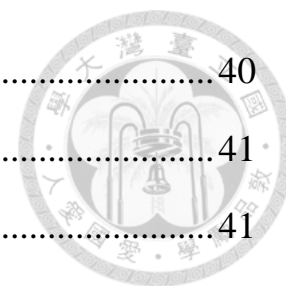
Table of contents

List of Figures

List of Tables

1. Introduction

1.1. Global aging leads to increasing prevalence of neurodegenerative diseases

The global population is aging rapidly. According to the Population Division of the United Nations Department of Economic and Social Affairs, World Population Ageing reports that by 2050, the proportion of individuals aged 60 and above will surpass 20% (Appendix 1). As the aging population continues to grow, so does the prevalence of various chronic diseases, including arthritis, heart disease, cancer, diabetes, chronic obstructive pulmonary disease, and notably, neurodegenerative diseases (Hou et al., 2019; Macnee et al., 2014) (Appendix 2).

Among the multitude of neurodegenerative diseases, Alzheimer's disease (AD) stands out as the most prevalent. It affects more than 100 out of 1,000 individuals aged 85 and above (Hou et al., 2019). Unfortunately, there is currently no known cure for neurodegenerative diseases.

1.2. Normal brain aging drives the progressive impairment of cognitive, social and physical abilities through various aspects

Throughout the aging process, histological alterations occur in neurons, glial cells, synapses, and myelin sheaths. These changes encompass the formation of plaques and tangles in neurons, reduced concentrations of nerve growth factors, chronic inflammation resulting in microglial activation, decreased neurotransmitter levels, impaired synaptic plasticity, demyelination, and gliosis. These age-related modifications in the brain are accompanied by behavioral impairments, including cognitive and psychiatric deficits, disrupted sleep patterns, and dysfunction in circadian rhythm, all of which significantly impact the individual's quality of life (Satoh et al., 2017) (Appendix 3).
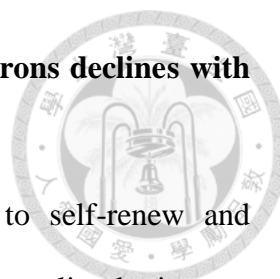
1.3. The capacity of NSCs to proliferate and generate new neurons declines with age

In the adult brain, NSCs possess the remarkable ability to self-renew and differentiate into both neurons and glial cells. Within the adult mammalian brain, two main reservoirs of active NSCs exist: the dentate gyrus (DG) in the hippocampus and the subventricular zone (SVZ) of the lateral ventricle. These regions house quiescent NSCs (qNSCs), which have the potential to proliferate and differentiate into new neurons and glial cells when activated, transforming into activated NSCs (aNSCs). However, it is important to note that adult neurogenesis undergoes a decline as part of the natural aging process, while neurodegeneration becomes more prevalent (Negredo et al., 2020) (Appendix 4).

There are several reasons contributing to this age-related decline in neurogenesis. Firstly, aged qNSCs exhibit reduced responsiveness to activation signals, making their transition into aNSCs more challenging (Audesse & Webb, 2020; Lugert et al., 2010). Additionally, the overall number of NSCs decreases as we age, further contributing to the decline in neurogenesis (Ibrayeva et al., 2021; Juan et al., 2011; Maslov et al., 2004).

1.4. The functional aging of SVZ is linked to neurodegenerative diseases

SVZ hosts the most extensive population of NSCs in rodents. When qNSCs within SVZ become activated, they rapidly undergo proliferation and subsequently differentiate into neuroblasts. These developing neuroblasts travel in groups along the rostral migratory stream (RMS) towards the olfactory bulb (OB). Once there, they seamlessly blend into the existing neural circuitry. (Bond et al., 2015; Cutler & Kokovay, 2020). This process has been demonstrated to play a crucial role in olfactory functions, including memory and the ability to discriminate scents and pheromones (Bragado Alonso et al.,

2
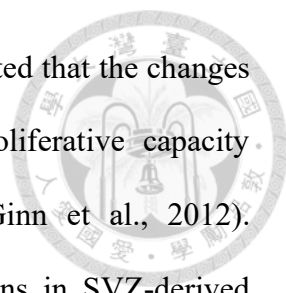
2019; Breton-Provencher et al., 2009; Cutler & Kokovay, 2020)

Furthermore, the functions of SVZ are intricately linked to neurodegenerative diseases. In mouse models, it has been observed that amyloid-β (Aβ), which is a peptide that plays a central role in AD, hinders the proliferation of adult NSCs derived from the SVZ (Esteve et al., 2022; Kim et al., 2022). While the precise role of SVZ adult neurogenesis in the human brain remains incompletely elucidated, research conducted on AD patients or cell lines derived from these patients has revealed that SVZ neurogenesis also plays a role in the mechanisms of neurodegenerative diseases. Interestingly, despite AD is a neurodegenerative disease, the population of neural progenitor cells (NPCs) originating from the SVZ is elevated in AD patients when compared to the healthy group (Kim et al., 2022; Mastroeni et al., 2016). Hence, additional investigations are required to elucidate the influence of aging in the SVZ on neurodegenerative conditions.

1.5. Age-related proteostasis imbalance in SVZ is likely to contribute to the diminished proliferative capacity of NSCs

Due to the crucial role of SVZ in the aging process, scientists have endeavored to explore various aspects of SVZ alterations. Of particular significance are the intrinsic factors of SVZ. A study employing RNA-sequencing (RNA-Seq) to characterize aging SVZ has unveiled a reduction in the expression of genes associated with neurogenesis, proliferation, and the cell cycle (Apostolopoulou et al., 2017). In more recent studies, researchers employed single-cell RNA-sequencing (scRNA-Seq) to characterize NSCs from both young and aged individuals. This approach unveiled differences in inflammation-related signatures. (Kalamakis et al., 2019).
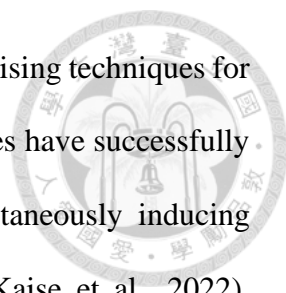
In contrast to the transcriptome, the proteome offers insights into protein levels, which directly aid in understanding protein functions and metabolism. Silver-stained 2-D

3

gels depicting age-related changes in the SVZ proteome have indicated that the changes in protein expression are likely responsible for the reduced proliferative capacity observed in stem/progenitor cells within the aging brain (McGinn et al., 2012). Additionally, quantitative proteomic analysis of age-related proteins in SVZ-derived neurospheres from young (7-day, 1-mo.) and middle-age (12-mo.) mice associated with neurodegenerative diseases such as AD and Parkinson's diseases (PD) has been conducted in neurosphere (Wang et al., 2016). In addition, lysosomal impairment has been identified as a contributor to diminished neurogenesis in the aging process. Research by Audesse and Webb in 2018 highlights that enhancing lysosomal performance can effectively rejuvenate stem cell function in the elderly brain (Audesse & Webb, 2018). However, our current knowledge regarding the proteomic changes in adult NSCs during the aging process remains limited.

1.6. The increase in neurodegenerative diseases, coupled with a decrease in adult neurogenesis, may be a reversible process

Traditionally, neuroscience held the belief that neurons, once lost, could not be regenerated, resulting in irreversible damage. For instance, the death of dopamine neurons contributes to PD, leading to the deterioration of motor function. Similarly, AD causes the demise of neurons crucial for cognition and memory, resulting in a decline in cognitive abilities. Unfortunately, effective treatments for these diseases are still lacking. However, in the 1960s, Altman and his team proposed the existence of neurogenesis in adult rats, although this concept was not widely accepted at the time (Altman & Das, 1965). It was not until the successful isolation and cultivation of NSCs in the 1990s that the field of neuroregenerative medicine began to flourish (Reynolds & Weiss, 1992; Richards et al., 1992).

Current research in animal models has demonstrated several promising techniques for potentially reversing neurodegenerative diseases. For instance, studies have successfully rejuvenated 20-month-old NSCs to a 1-month-old state by simultaneously inducing *PlagI2* expression and knocking down *Dyrk1a* using lentivirus (Kaise et al., 2022). Furthermore, CRISPR-mediated in vivo central nervous system (CNS) gene editing via AAV has shown promise in the field of reversing neurodegenerative diseases (Xiao et al., 2021). Additionally, the transplantation of new NSCs has emerged as a potential avenue for intervention (Marqués-Torrejón et al., 2021). These groundbreaking studies have sparked tremendous excitement, as they provide the possibility of reversing neurodegenerative diseases.

1.7. Protein N-terminal modification, especially N-terminal acetylation, may play important roles in aging and pathological neurodegeneration

Maintaining proteostasis entails a intricate network of pathways that impact the destiny of a protein from its creation to eventual degradation. Maintaining the balance of proteostasis through the N-terminus is noticeable across a spectrum of organisms found in different biological realms. Various modifications to the N-terminal amino acids play a crucial role in shaping protein function, directing their targeting, and influencing stability in diverse manners. (Dissmeyer et al., 2019).

There's strong evidence indicating that protein N-terminal acetylation could be crucial for aging and pathological degeneration (Rope et al., 2011). N-terminal acetylation is carried out by the N-a-acetyltransferase (NAT) family which in cytoplasm co-translationally acetylates the first aa of 80-90% of human proteins. The NAT family consists of six complexes: NatA, NatB, NatC, NatD, NatE, and NatF. Each complex has its own distinctive catalytic subunit, and some also feature a unique ribosomal anchor that

plays a role in substrate specificity. Notably, the S37P mutation in Naa10p, associated with Ogden syndrome, has been linked to premature aging in human patients (Rope et al., 2011). Additionally, studies in yeast have revealed that Naa40p, another protein involved in histone N-terminal acetylation, plays a regulatory role in lifespan (Steffen et al., 2008). Despite these findings, our understanding of how N-terminal acetylation of histones and non-histone proteins specifically mediates the aging and pathological degeneration of NSCs remains incomplete.

2. Results

2.1. The most effective adult neurosphere culture system was established

SVZ and DG contain highly heterogeneous cell populations that play critical roles in neurogenesis, ranging from upstream NSCs to differentiated mature neurons and macroglia. To investigate the differences between aging NSCs and their younger counterparts and to gain insights into the potential factors contributing to the aging process, we established an advanced in vitro culture system for adult NSCs. Currently, there are various widely used methods for culturing NSCs, but the efficiency of these cultures varies. There has yet to be a comprehensive comparison of these widely used methods. Therefore, we aim to establish an optimized in vitro adult NSCs culture system as a preliminary step for our subsequent studies.

2.1.1. The age of the mice was chosen based on the corresponding human age

In accordance with the life phase equivalences established for mice and humans (Kevin Flurkey, 2007) (Appendix 5), our study involved the selection of two distinct age groups. The aged group consisted of 18-22-month-old female mice, which is biologically equivalent to the aging range of 56-69 years in humans. For the young group, we utilized

2-3-month-old female mice, reflecting an age range of 20-30 years in humans. This specific age range was chosen to enable the examination of the natural aging progression in mice, closely mirroring the aging trajectory observed in humans.
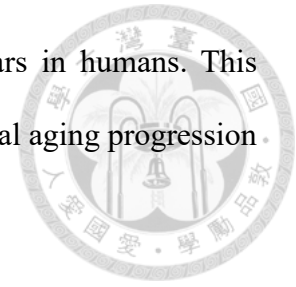
2.1.2. Cells from SVZ of both young and old mice were isolated

To culture NSCs, we extracted brains from both old and young mice (Fig. 1A). First, we coronally sliced the brain along the optic nerve to expose the sections of SVZ (Fig. 1B). Subsequently, we isolated regions enriched with NSCs from the SVZ (Fig. 1C), following established protocols (Ahmed et al., 2021; Hagihara et al., 2009). The isolated tissues were sliced with a blade and then digested using accutase to obtain single cells. Afterward, these cells were washed with a wash medium to obtain purified primary NSCs, which were utilized for conducting neurosphere assays. Details are described in the Materials and Methods section
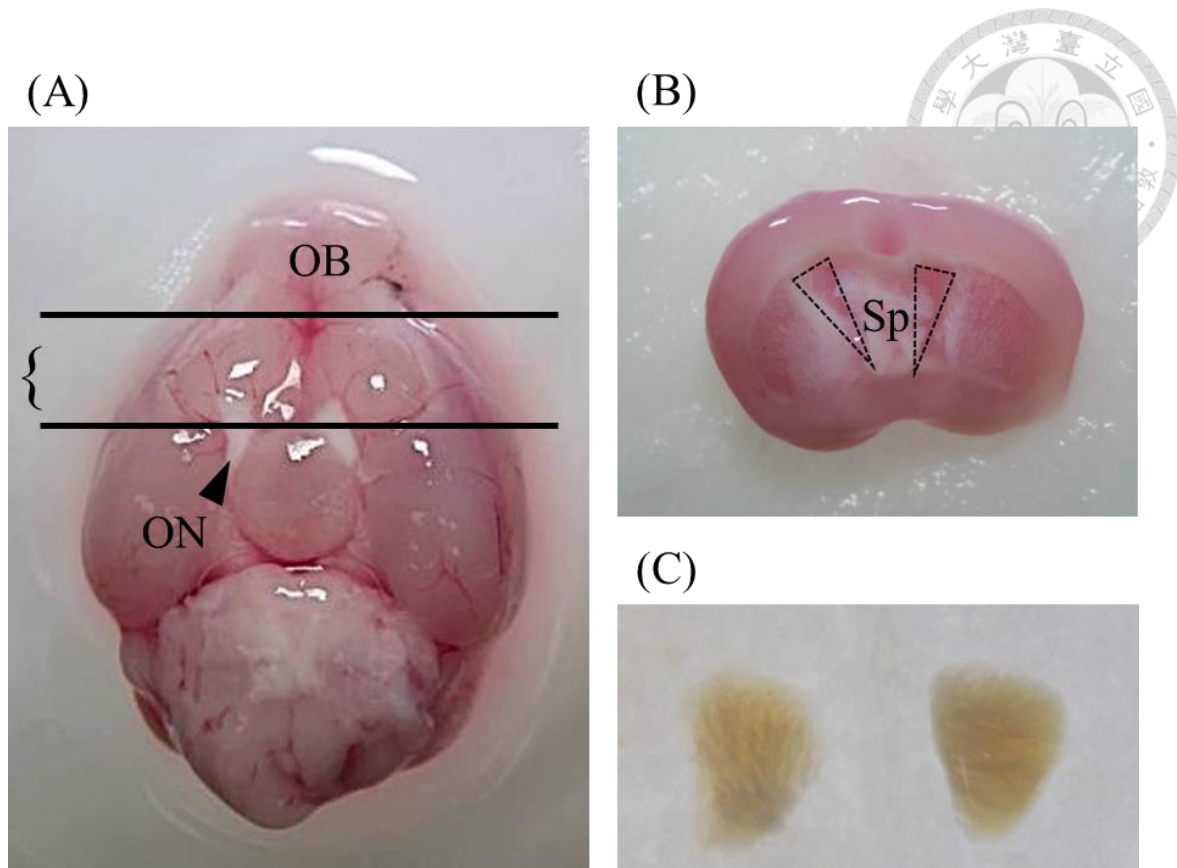
Figure 1. SVZ tissue was isolated from the adult mouse brain.

(A) Dorsal view of a brain from a young mouse (2-mo.). The brain was coronally sliced along the optic nerve (ON) to expose SVZ. The areas between the black lines correspond to the sections for SVZ isolation. **(B)** Coronal section from (A) revealed SVZ. The black dashed lines outline SVZ. Subsequently, the septal area (Sp) is removed, and SVZ is isolated along the black dashed lines. **(C)** Isolated SVZ tissue. The tissue can be digested for NSC culture. OB, olfactory bulb; ON, optic nerve; Sp, septal area.

2.1.3. The optimized neurosphere culture medium was selected from the currently commonly used media

The neurosphere assay is a widely utilized suspension culture system for assessing the presence of NSCs (Soares et al., 2021). In this method, cells are suspended in ultra-low adherent culture dishes and grown in a culture medium enriched with essential growth factors such as EGF and FGF. After 3-5 days of culture, these NSCs aggregate to form distinct three-dimensional structures known as neurospheres. This innovative technique provides a valuable means to study and characterize NSCs in vitro, making it an indispensable tool in neuroscience research.

However, despite the abundance of published culture media formulations for neurosphere formation, there is a noticeable lack of comprehensive comparative studies rigorously assessing their performance. This knowledge gap poses a significant challenge in the field of stem cell research, hindering our ability to determine the optimal culture medium composition for specific experimental goals. Therefore, we initiated a screening process to identify the most efficient culture medium for neurosphere formation from a pool of 21 distinct formulations (M1-M21) (Table 1). These formulations encompass three basal media options, namely DMEM-F12, neural basal medium (NB), and neural stem cell basal medium (NSCBM), each supplemented with either N2 or B27, or a combination of both.
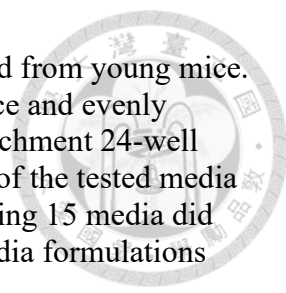
Table 1. The list of media tested in the thesis.

Medium#	Basal medium	Alternative supplement	References	Supplement
M1	DMEM/F12	1% N2	(Wachs et al., 2003)	1x GlutaMax, 1x primocin, 20 ng/ml EGF and 20 ng/ml FGF
M2	DMEM/F12	2% B27	(Ahlenius et al., 2009; Wachs et al., 2003)	
M3	DMEM/F12	0.5% N2+ 1% B27	(Kim et al., 2016)	
M4	NB	1% N2	(Wachs et al., 2003)	
M5	NB	2% B27	(Kalamakis et al., 2019; Wachs et al., 2003; Walker & Kempermann, 2014)	
M6	NB	0.5% N2+ 1% B27	(Wachs et al., 2003)	
M7	NSCBM	1% N2	Non	
M8	NSCBM	2% B27	(Ahmed et al., 2021)	
M9	NSCBM	0.5% N2+ 1% B27	Non	
M10	DMEM/F12+NB (1:1)	1% N2	Non	
M11	DMEM/F12+NB (1:1)	2% B27	Non	
M12	DMEM/F12+NB (1:1)	0.5% N2+ 1% B27	(Goffredo et al., 2008; Lee et al., 2020)	
M13	DMEM/F12+NSCBM (1:1)	1% N2	Non	
M14	DMEM/F12+NSCBM (1:1)	2% B27	Non	
M15	DMEM/F12+NSCBM (1:1)	0.5% N2+ 1% B27	Non	
M16	NB+NSCBM (1:1)	1% N2	Non	
M17	NB+NSCBM (1:1)	2% B27	Non	
M18	NB+NSCBM (1:1)	0.5% N2+ 1% B27	Non	
M19	DMEM/F12+NB+NSCBM (1:1:1)	1% N2	Non	

NB, neural basal medium; NSCBM, neural stem cell basal medium

Initially, we conducted tests on culture media using SVZ cells derived from young mice. Cells were obtained by pooling SVZ tissue from six 2-month-old mice and evenly distributed across the 21 different culture media within ultra-low attachment 24-well plates (Sigma-Aldrich). Following a 7-day incubation period, only six of the tested media exhibited neurosphere with a diameter >500 μm (Fig. 2). The remaining 15 media did not exhibit noticeable neurosphere formation. These six effective media formulations consisted of the following:

1. M2: DMEM-F12 supplemented with B27

2. M6: Neural basal medium (NB) with a 1:1 mixture of N2 and B27

3. M11: A 1:1 mixture of DMEM-F12 and NB with B27

4. M12: A 1:1 mixture of DMEM-F12 and NB with a 1:1 mixture of N2 and B27

5. M14: A 1:1 mixture of DMEM-F12 and neural stem cell basal medium (NSCBM) with a 1:1 mixture of N2 and B27

6. M21: A 1:1:1 mixture of DMEM-F12, NB, and NSCBM with a 1:1 mixture of N2 and B27.

It is important to note that the listed components only contain the different components among the media; modifications were made exclusively to the compositions of the basal medium and supplements. Other components such as GlutaMAX, antibiotics, and so forth, were included as detailed in the materials and methods section.

After confirming the ability of these six selected media to generate neurospheres, newly formed small neurospheres in these cultures were directly transferred to ultra-low attachment 24-well plates (Sigma-Aldrich) to provide sufficient space for growth. This step aimed to assess whether neurospheres could sustain proliferation and enlarge further. Following an additional 7 days of culture, with the exception of M2 (DMEM-F12 supplemented with B27), neurospheres cultured in the other five media exhibited notable growth, indicating that these five media formulations not only support neurosphere

11

formation but also have the potential for expansion. Consequently, we replicated neurosphere cultures using these five promising media formulations and enhance the efficiency of neurosphere formation by increasing cell density. Cells were maintained in ultra-low attachment 24-well plates. After one week, the number and size of the generated neurospheres were quantified.

The results revealed that M11, M12, and M21 generated neurospheres with the largest diameter (µm), among which, M11 and M12 produced the highest number of neurospheres (per cm²) (Fig. 3 and Table. 2). Taking cost into consideration, we selected M12 (1:1 mixture of DMEM-F12 and NB with a 1:1 mixture of N2 and B27) as the optimized neurosphere culture medium for subsequent experiments.

(A)

Tissue dissection — Transfer and add medium

24 well — 6 well

Day0 — Day7 — Day14

(B)

Day 0

	DMEM-F12	Neural basal	NSCBM	DMEM-F12 + NB	DMEM-F12 + NSCBM	NB + NSCBM	DMEM-F12 + NB + NSCBM
N2	M1	M4	M7	M10	M13	M16	M19
B27	M2	M5	M8	M11	M14	M17	M20
N2+B27 (1:1)	M3	M6	M9	M12	M15	M18	M21

500 µm

(C)

Day 7

	DMEM-F12	Neural basal	NSCBM	DMEM-F12 + NB	DMEM-F12 + NSCBM	NB + NSCBM	DMEM-F12 + NB + NSCBM
N2	M1	M4	M7	M10	M13	M16	M19
B27	M2	M5	M8	M11	M14	M17	M20
N2+B27 (1:1)	M3	M6	M9	M12	M15	M18	M21

500 µm

(D)

Day 14

	DMEM-F12	Neural basal	NSCBM	DMEM-F12 + NB	DMEM-F12 + NSCBM	NB + NSCBM	DMEM-F12 + NB + NSCBM
N2	M1	M4	M7	M10	M13	M16	M19
B27	M2	M5	M8	M11	M14	M17	M20
N2+B27 (1:1)	M3	M6	M9	M12	M15	M18	M21

200 µm

13

Figure 2. M6, M11, M12, M14, and M21 exhibited neurospheres with a diameter >500 μm after 14 days of culture.

(A) Schematic showing the testing of different culture media for neurosphere formation. (B-D) Neurospheres cultured using 21 different culture media. Cells were derived from SVZ of six young mice (2.5 mo.). NB, neural basal medium; NSCBM, neural stem cell basal medium. Representative images of cells on (B) day 0, (C) day 7, and (D) day 14 are shown, with red boxes indicating the formation of at least one neurosphere with a diameter >500 μm.
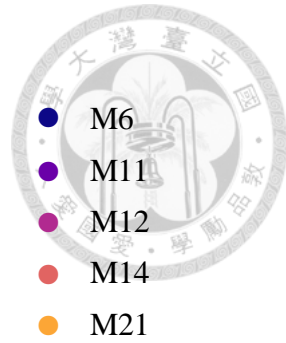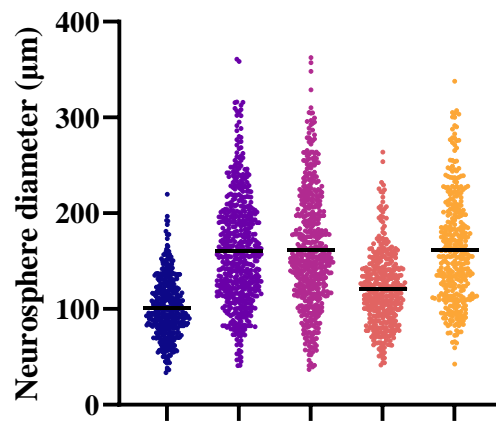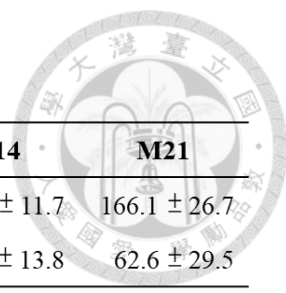
DMEM-F12	-	+	+	+	+
Neurobasal medium	+	+	+	-	+
Neural stem cell basal medium	-	-	-	+	+
B27	+	+	+	+	+
N2	+	-	+	+	+

Figure 3. M11, M12 and M21 are the most efficient neurosphere culture media.

Five media with at least one neurosphere with a diameter >500 μm were selected and used for subsequent culturing. Cells were derived from SVZ of six young mice (2.5 mo.) pooled together. Neurosphere counts and sizes were measured after 7 days of culture, with the experiment conducted in triplicate (n=3). The black horizontal bar represents the average size of all neurospheres from triplicate measurements.

Table 2. Neurosphere counts and sizes of selected five media.

	M6	M11	M12	M14	M21
Neurosphere size (μm)	102.1 ± 10.2	162.1 ± 22.7	158.6 ± 27.0	118.9 ± 11.7	166.1 ± 26.7
Total number (/cm^2)	75.4 ± 15.9	91.1 ± 13.9	89.6 ± 9.8	68.2 ± 13.8	62.6 ± 29.5

The results are presented as the mean ± SD from three experiments conducted in triplicate.

2.2. NSCs were characterized within our culture system

2.2.1. Cells in adult SVZ-neurospheres expressed NSC markers

To confirm the existence of NSCs within the neurospheres, neurospheres were enzymatically digested and subjected to monolayer culture. Immunofluorescence (IF) staining demonstrated that cells in neurospheres from old mice (21-mo.) express the NSC markers Nestin (Fig. 4A) and Vimentin (Fig. 4B), providing evidence for the presence of NSCs within the neurospheres.

2.2.2. Cells in adult SVZ-neurospheres exhibited differentiation

In addition to the expression of NSC marker, NSCs are recognized for their self-renewal and multipotent nature, contribute to the generation of neurons and glial cells in both embryonic and adult brains (Angata & Fukuda, 2010). As neurosphere-forming cells exhibit the capability of self-renewal, the formation of neurospheres is commonly considered as an indication of their status as stem cells (Mich et al., 2014).

On the other hand, to validate the differentiation potential of cells within neurospheres in our culture system, we enzymatically digested the neurospheres into single cells for monolayer cultivation. After one day of cultivation in NSC growth medium, we switch to a medium without EGF and FGF to induce cellular differentiation (Donato et al., 2007). Three days later, IF analysis was conducted to evaluate the cell types. The staining revealed the presence of the mature neuron marker Tuj1 (Fig. 5A) and the astrocyte marker GFAP (Fig. 5B), illustrating the capacity of cells in SVZ-neurospheres from the adult mice to differentiate into neurons and glial cells. This evidence indicates the presence of NSCs in SVZ-neurospheres in our culture system.
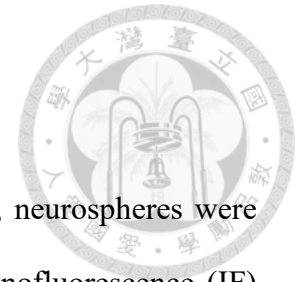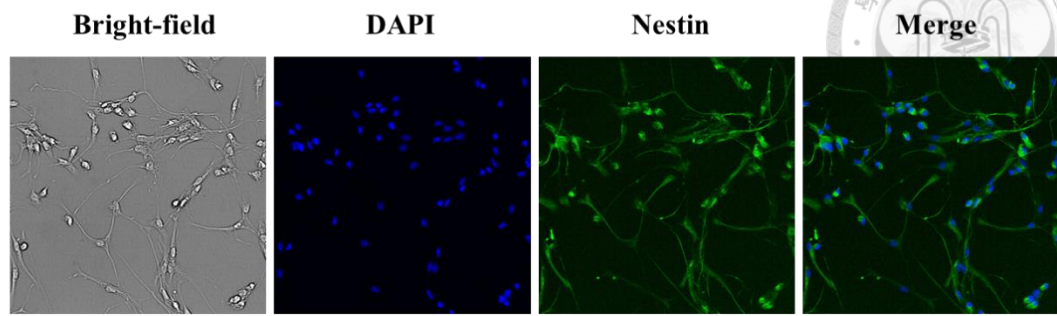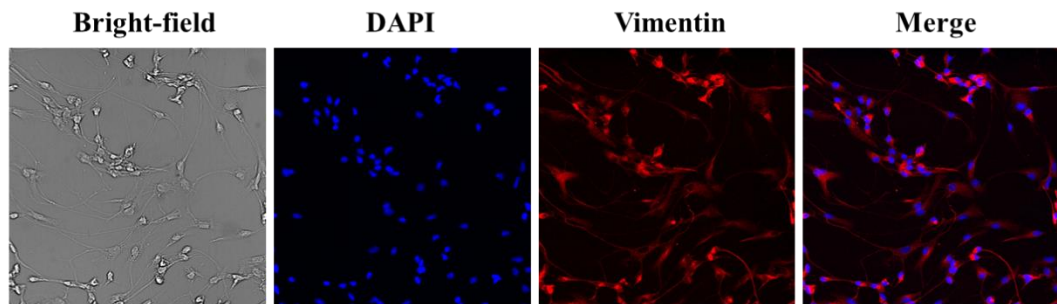
Figure 4. Cells in adult SVZ-neurospheres expressed NSC markers.

IF was performed on cells from SVZ-neurospheres derived from old (21 mo.) mice. The cells were stained for NSC markers, including **(A)** Nestin (green) and **(B)** Vimentin (red). DAPI staining is represented in blue.

(A)

(B)

200 μm
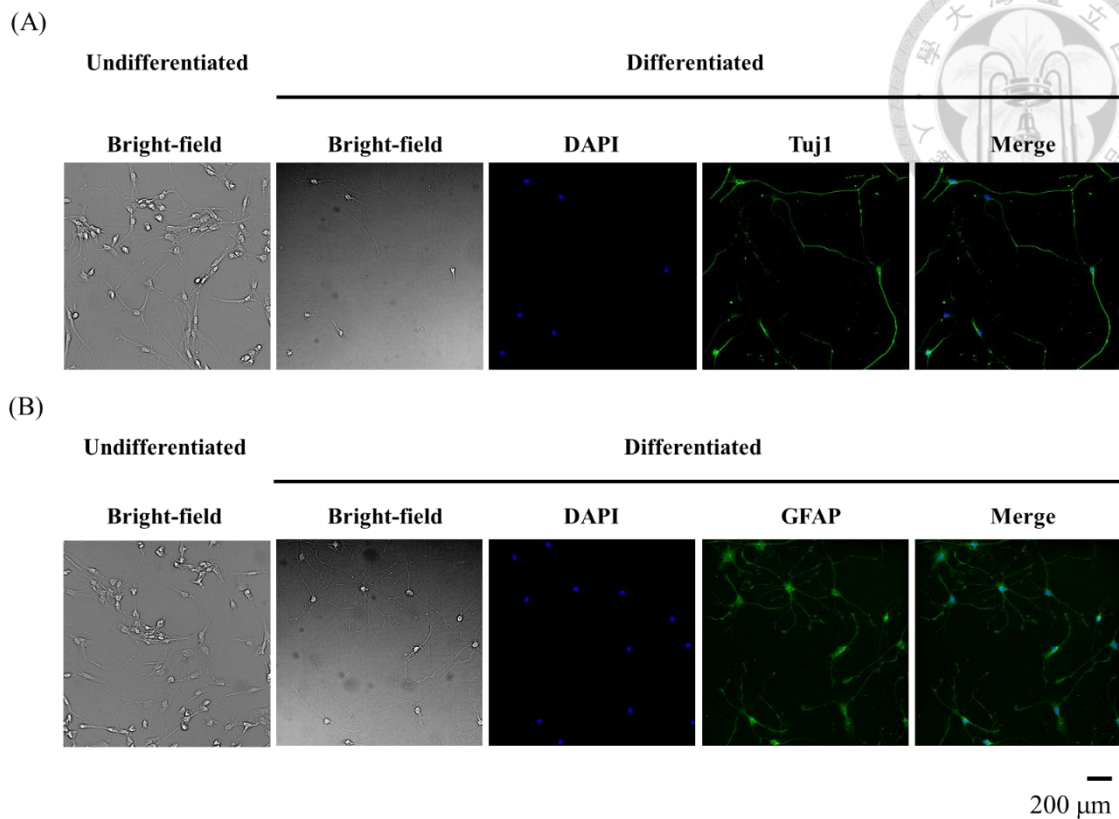
Figure 5. Cells in adult SVZ-neurospheres exhibited differentiation.
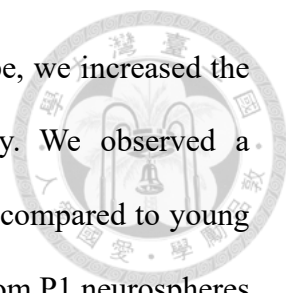
IF was performed on cells derived from SVZ-neurospheres of old (19 mo.) mice after differentiation. NSC growth medium was switched to EGF and FGF removal medium after one day of culturing to induce NSC differentiation for an additional three days. The cells were stained for the mature neuron marker **(A)** Tuj1 (green) and the astrocyte marker **(B)** GFAP (green). DAPI staining is represented in blue.

2.3. The impaired ability of SVZ NSCs from aged mice to form neurospheres could be sustained until P1 *in vitro* but is lost from P2 and beyond

Neurosphere-forming capability serves as a widely adopted and critical parameter for assessing adult neurogenesis. In order to explore the persistence of functional distinctions within the SVZ-neurospheres between young and old mice using this culture system, we conducted a comparative assessment of their neurosphere-forming capacity. Cells from SVZ tissues of both young (2 months old) and aged (20 months old) mice were isolated, enzymatically digested, and then seeded into ultra-low adherent 24-well plates for suspension culture, resulting in the formation of first-generation neurospheres (primary neurospheres). After 7 days, we quantified both the number and size of the neurospheres. Our findings revealed that SVZ-cells from young mice generated a significantly higher number of primary neurospheres compared to those from the old mice (Fig. 6A). Nevertheless, the distribution of primary neurospheres of different sizes exhibited similarity between the two age groups (Fig. 6B).

To determine the persistence of these differences through subsequent passaging, primary neurospheres were digested into single cells and passaged to suspension culture to generate second-generation neurospheres (passage-1, P1). After a 7-day incubation period, these P1 neurospheres were quantified. Consistent with the observations made for the primary neurospheres, SVZ cells from young mice formed more P1 neurospheres compared to those from old mice (Fig. 6A), while the size distribution remained consistent between the two age groups (Fig. 6C).

Notably, the reduced ability of aged SVZ cells to form neurospheres was only seen up to the P2 and did not continue afterward (Fig. 6A). These findings suggest that within our culture system, the functional disparities between SVZ cells from young and aged mice, especially in terms of neurosphere formation, can be sustained and preserved until

P1 but is lost from P2 and beyond. To further confirm this phenotype, we increased the sample size and concurrently assessed the proliferation capacity. We observed a significant decrease in P1 neurosphere forming ability in aged mice compared to young mice (Fig. 7A, B, and C). Notably, the proliferation ability for cell from P1 neurospheres was reduced in aged mice when compared to their younger counterparts (Fig. 7D), without affecting their survival rate (Fig. 7E).   Since age-related protein-NAc change in SVZ is likely to contribute to the diminished proliferative capacity of NSCs, we next conducted LC-MS/MS to comprehensively analyze the alteration of the protein-NAc change in P1 neurospheres from young and old mice.

(A)

(B)

Primary

(C)

P1
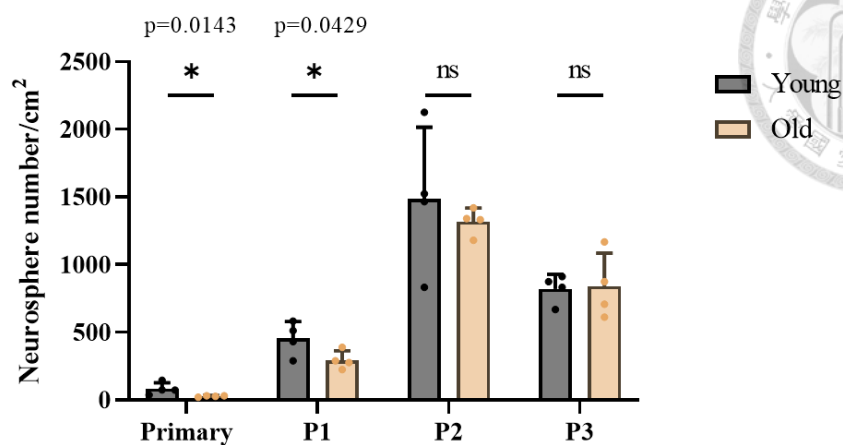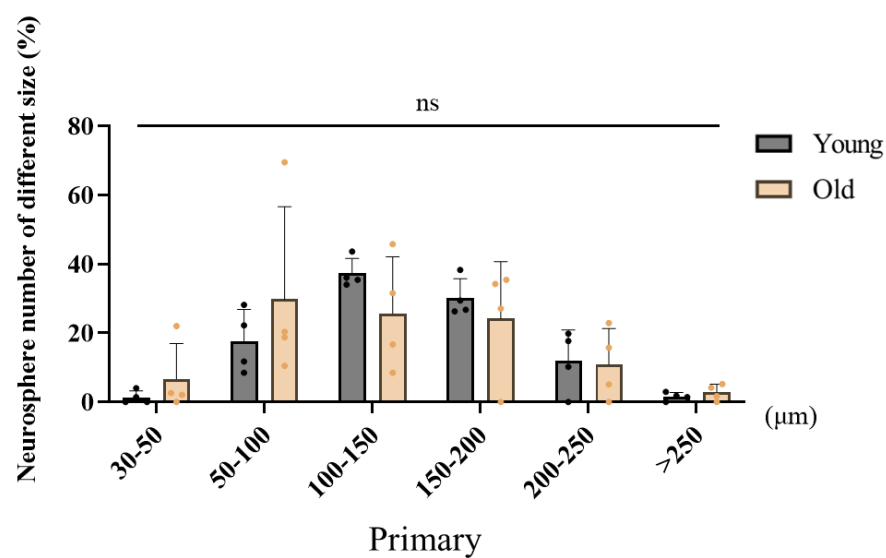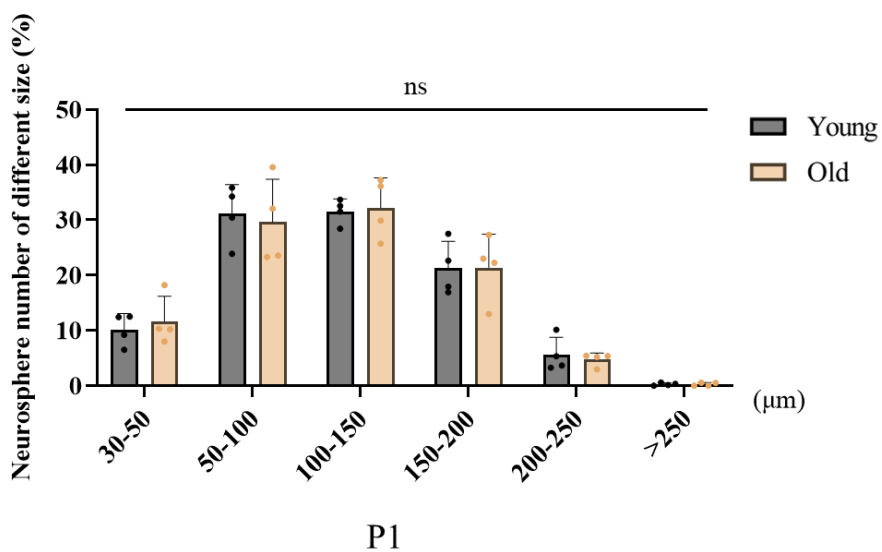
Figure 6. The impaired ability of SVZ NSCs from aged mice to form neurospheres could be sustained until P1 *in vitro* but is lost from P2 and beyond.

(A) The number of neurospheres formation of aged mice (20 mo., n=4) and young mice (2 mo., n=4). The counts were measured after 7 days of culture and normalized to cm^2. Proportions (%) of primary **(B)** and P1 **(C)** neurospheres of different sizes measured from (A). Error bars represent the standard deviation. Significance levels were determined using Student's t-test (*p < 0.05). NS, not significant.
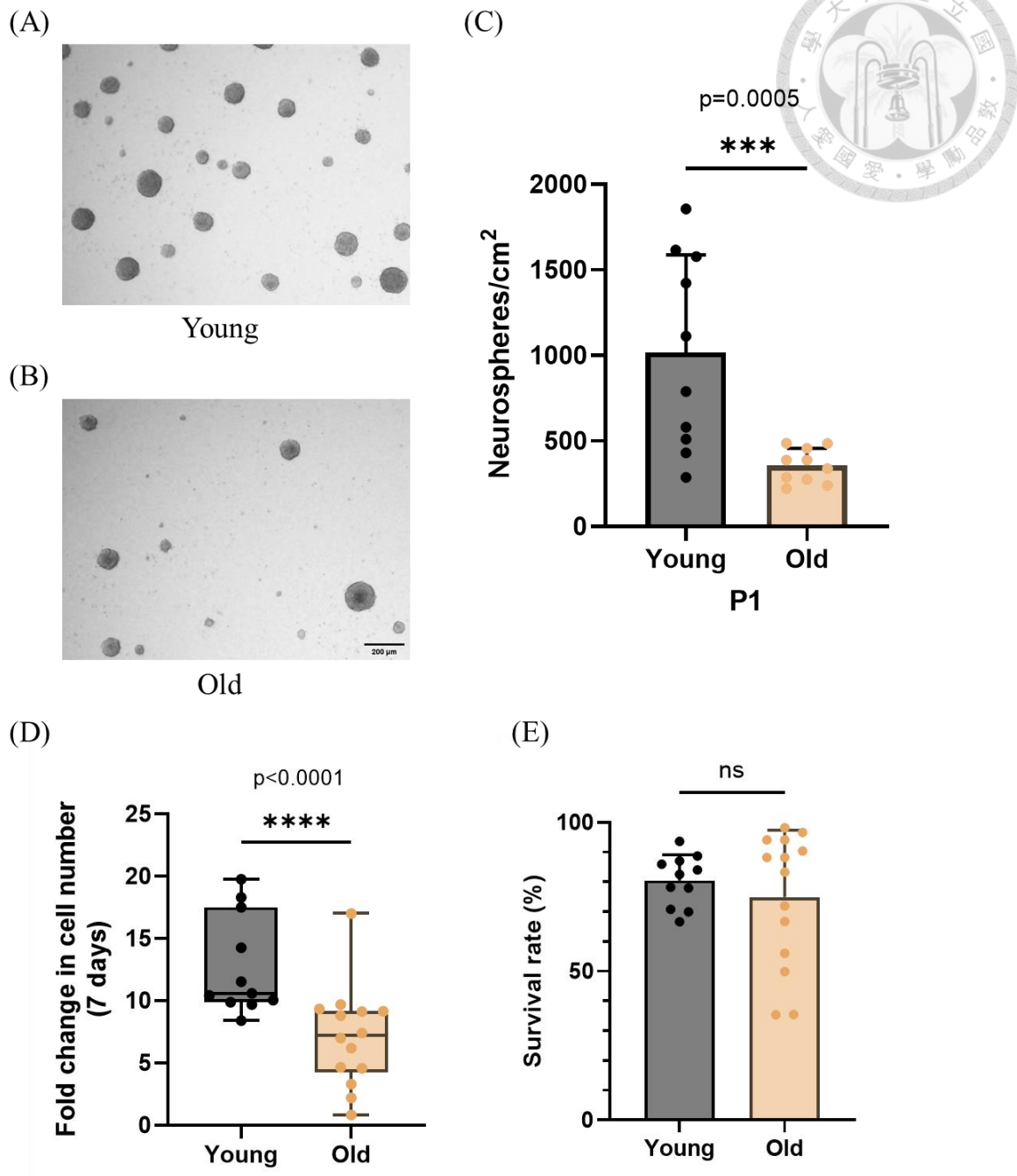
Figure 7. The neurosphere formation ability and proliferation capacity of P1 NSCs were reduced in older mice compared to young mice.

Representative images of young (2 mo.) **(A)** and aged (18 mo.) **(B)** P1 neurospheres. Scale bar=500 μm. **(C)** The number of P1 neurospheres of young mice (2 mo., n=10) and old mice (20-21 mo., n=10). The counts were measured after 7 days of culture and normalized to cm^2. **(D)** The fold change in NSC number of young (2 mo., n=11) and old

(21 mo., n=14) P1 neurosphere after 7 days culture. **(E)** Survival rate of NSCs from (D).

Error bars represent the standard deviation.

2.4. The dysregulation of protein N-terminal acetylation occurred in adult NSCs both in vitro and in vivo during aging

2.4.1. The proteomic analysis uncovered proteins with NAc ratios significantly increased or decreased between young and old mice

Using LC-MS/MS, we were able to obtain information about protein N-terminals from P1 neurospheres of 5 old (21 mo.) and 5 young (2 mo.) mice. In total, we identified 916 unique N-terminal peptides, out of which 896 had N-acetylation (NAc) ratios of 100%. Importantly, we observed significant differences in NAc ratios between young and old mice for specific proteins. We identified four proteins with their NAc ratio increased significantly in the old neurosphere. These four proteins are TMSB10 (Thymosin beta-10), PPIA (Peptidyl-prolyl cis-trans isomerase A), SLC6A11 (Sodium- and chloride-dependent GABA transporter 3), and PSMD1 (26S proteasome non-ATPase regulatory subunit1). In contrast, we found DDT (D-dopachrome decarboxylase), whose NAc ratio decreased with age.

Table 3. Proteins with NAc ratios significantly increased or decreased between young and old mice were identified through LC-MS/MS analysis.
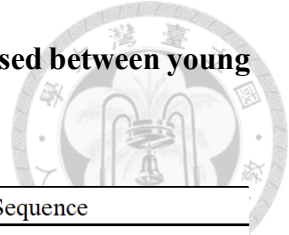
Name	Description	Sequence
Proteins with age-dependent increase in protein NAc levels ($p<0.05$)		
TMSB10	Thymosin beta-10	ADKPDMGEIASFDK
PPIA	Peptidyl-prolyl cis-trans isomerase A	VNPTVFFDITADDEPLGR
SLC6A11	Sodium- and chloride-dependent GABA transporter 3	TAEQALPLGNGKAAEEAR
PSMD1	26S proteasome non-ATPase regulatory subunit 1	MITSAAGIISLLDEEEPQLK
Proteins with age-dependent decrease in protein NAc levels ($p<0.05$)		
DDT	D-dopachrome decarboxylase	PFVELETNLPASR

(Continue from the upper table)

Name	Ac% young	Ac% old	p-value	Ac% change
Proteins with age-dependent increase in protein NAc levels ($p<0.05$)				
TMSB10	61.796±21.054	84.107±9.727	0.045	22.311
PPIA	13.460±5.710	20.868±4.752	0.005	12.408
SLC6A11	0.000±0.000	5.069±5.097	0.045	5.069
PSMD1	2.421±1.913	5.336±1.089	0.015	2.915
Proteins with age-dependent decrease in protein NAc levels ($p<0.05$)				
DDT	92.049±2.677	85.396±4.257	0.015	-6.653

Protein N-terminals were derived from P1 neurospheres of young (2 mo., n=5) and old (21 mo., n=5) mice. Ac%, ratio protein N-α-acetylation. Table shows mean Ac%±SD. Proteins are sorted in descending order based on the degree of change in NAc ratio.

2.4.2. The amount of protein free N-termini in NSCs from SVZ decreased during aging

To explore the potential connection between the differential neurosphere-forming abilities of SVZ cells from young and aged mice and protein acetylation, we conducted an analysis of protein free N-terminal levels in P1 neurospheres. We employed the NBD-Cl (4-chloro-7-nitrobenzofurazan) assay (Ree et al., 2018). This method involves the treatment of native proteins with the fluorescent NBD-Cl dye, which forms a fluorescence-emitting complex upon binding to primary amines under neutral pH conditions. Consequently, stronger fluorescence signals indicate higher levels of protein free N-termini, suggesting a lower level of protein NAc.

We extracted total protein lysates from both young and old SVZ P1 neurospheres, followed by incubation with NBD-Cl. The results revealed that the aged group exhibited relatively lower fluorescence levels, suggesting a lower level of protein free N-terminal acetylation in the aged P1 neurospheres (Fig. 8).
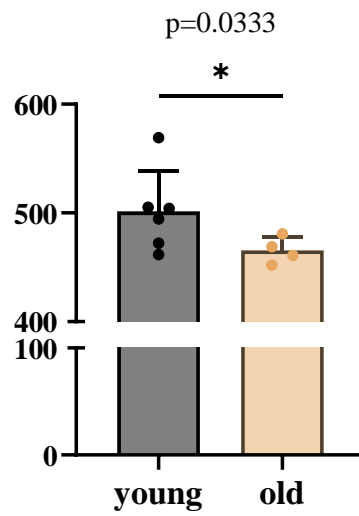
Figure 8. Protein free N-terminal level in NSCs from SVZ decreased during aging.

NBD-Cl assay was performed to quantify free N-terminal levels of total protein extracted from SVZ neurospheres of old (18-20 mo., n=4) and the young (2-3 mo., n=6) mice. Relative fluorescence was normalized to units per microgram of protein. Error bars indicate standard deviations.

2.4.3. mRNA levels of *Naa20* and *Naa35* were significantly higher in SVZ NSCs of aged mice

To identify the specific group of proteins with N-terminal acetylation influenced by aging and investigate their potential functional relevance to neurogenesis, RT-qPCR was employed to analyze the mRNA expression levels of ten members of the N-terminal acetyltransferase (NAT) family, namely NatA (*Naa10*, *Naa15*), NatB (*Naa20*, *Naa25*), NatC (*Naa30*, *Naa35*), NatD (*Naa40*), NatE (*Naa50*), NatF (*Naa60*) and *Naa80*. Each Nat enzyme exhibits specificity towards distinct substrate proteins. Therefore, identifying the Nat genes that show differential expression between aged and young mice may help narrow down the proteins affected by aging-associated changes.

Compared to young mice (2 mo.), mRNA levels of *naa20* and *naa35* were significantly higher in neurospheres from old mice (21 mo.) (Fig. 9). Referring to our previous discovery of the increased global N-terminal acetylation in aged neurospheres, we speculate that the substrate proteins of *Naa20* and *Naa35* might be the candidates contributing to this phenomenon.
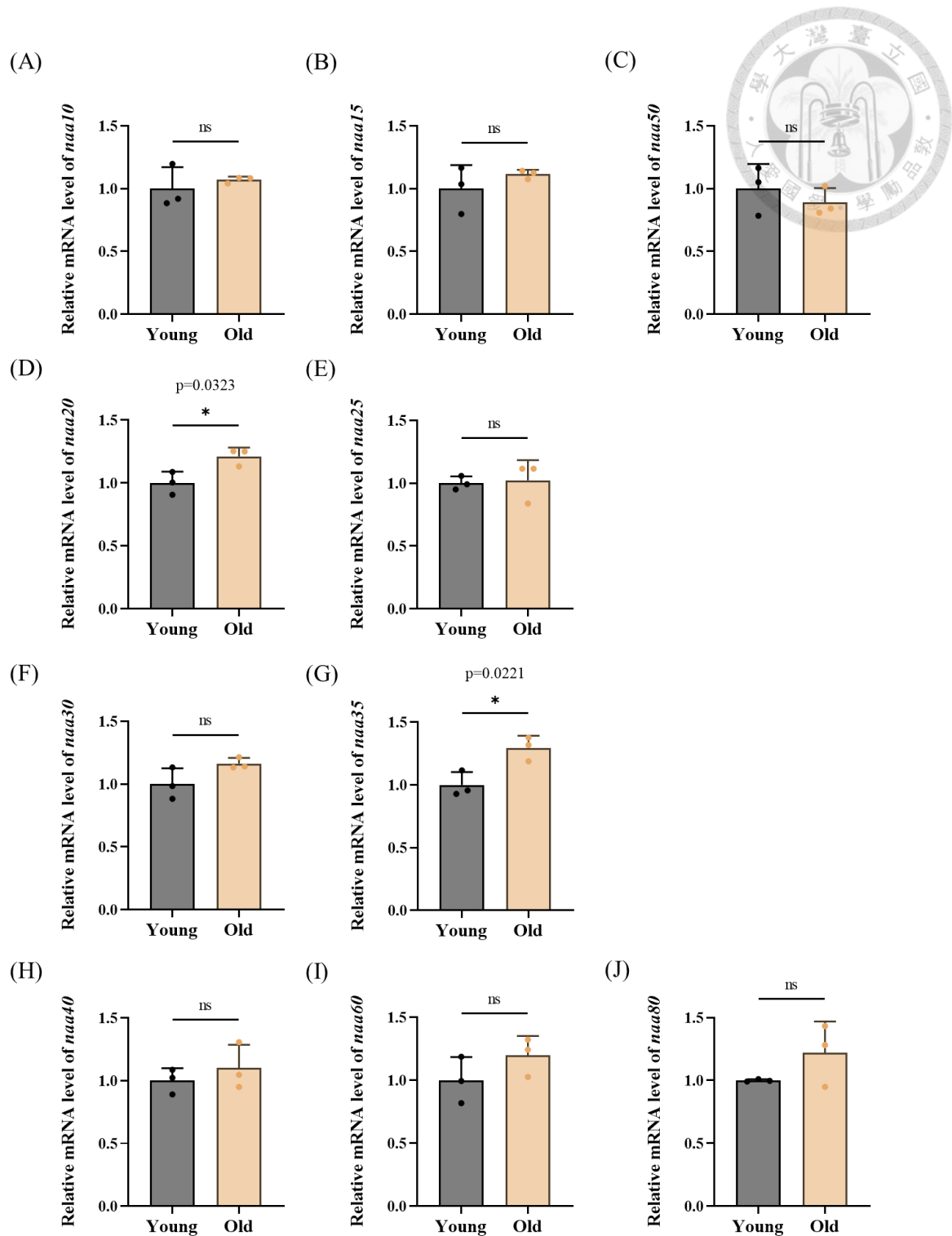
Figure 9. mRNA levels of *Naa20* and *Naa35* are significantly higher in SVZ NSCs of aged mice.

RT-qPCR analysis was used to investigate the mRNA levels of 10 Nat genes in SVZ P1 neurospheres of young (2 mo., n=3) and old mice (21 mo., n=3). The $2^{-\Delta\Delta CT}$ method was

31

employed to assess the relative mRNA levels by normalizing them to *gapdh* expression

and then expressing them relative to the levels in young mice. Error bars represent the

standard deviations.
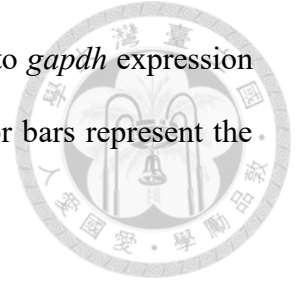
2.4.4. Protein free N-terminal level was altered specifically in different brain regions during aging

Since we have observed that aged neurospheres exhibit reduced formation capacity and lower levels of protein free N-termini, it raises the possibility of a connection between protein free N-termini and the decline in adult neurogenesis with aging. To more directly validate this hypothesis, we extracted total protein lysates from the SVZ of both aged and young mice and conducted the NBD-Cl experiment. Consistently, we found that the SVZ of old mice (18-20 mo.) displayed lower fluorescence intensity, indicating lower protein free N-terminal levels compared to young mice (2-3 mo.) (Fig. 10A). This aligns with the findings in SVZ P1 neurospheres, suggesting that protein free N-terminal holds physiological significance and may be associated with the decline in neurogenesis during aging. Nevertheless, it is important to note that no similar decrease in protein free N-terminal level was detected in the DG region (Fig. 10B). These findings suggest that protein free N-termini undergo region-specific alterations during the aging process, with the SVZ being particularly susceptible to decreased free N-termini.
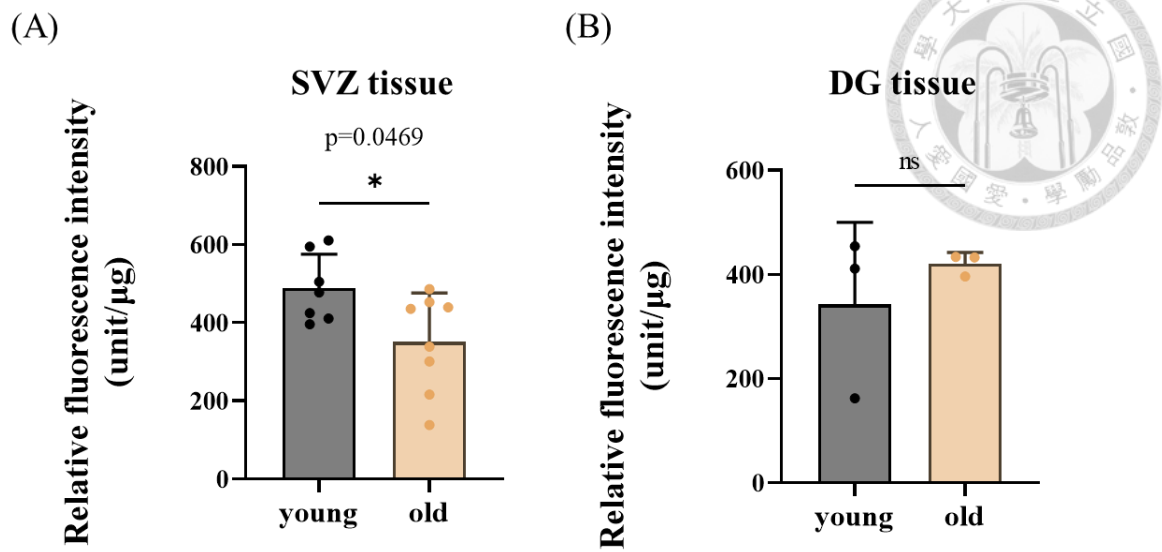
Figure 10. Protein free N-terminal level was altered specifically in different brain regions during aging.

NBD-Cl assay was performed to quantify free N-terminal levels of total protein extracted from **(A)** SVZ tissue of young (2-3 mo., n=7) and aged (18-20 mo., n=8) mice or from **(B)** DG tissue of young (2-3 mo., n=3) and aged (18-20 mo., n=3) mice. Relative fluorescence was normalized to units per microgram of protein. Error bars indicate standard deviations.

2.4.5. mRNA levels of Nat genes altered specifically in different brain regions during aging

In the context of the 10 Nat genes, RT-qPCR reveals a significant increase in the mRNA levels of *Naa15* and *Naa80* in SVZ of aged mice (19-20 mo.) compared to young mice (2-3 mo.) (Fig. 11B and J). However, no age-related changes were observed in the expression of other Nat genes (Fig. 11). This provides a potential explanation for the observed increase in the protein global N-terminal acetylation level in the SVZ with aging. Conversely, although the protein global N-terminal acetylation level in DG does not change with age, when examining the expression of Nat genes in the DG, we observed a notable upregulation of *Naa15* (Fig. 12A), *Naa20* (Fig. 12D), and *naa80* (Fig. 12J) in aged mice. This indicates region-specific differences in protein N-terminal acetylation, highlighting the complexity and specificity of the regulatory mechanisms involved in acetylation processes during aging.
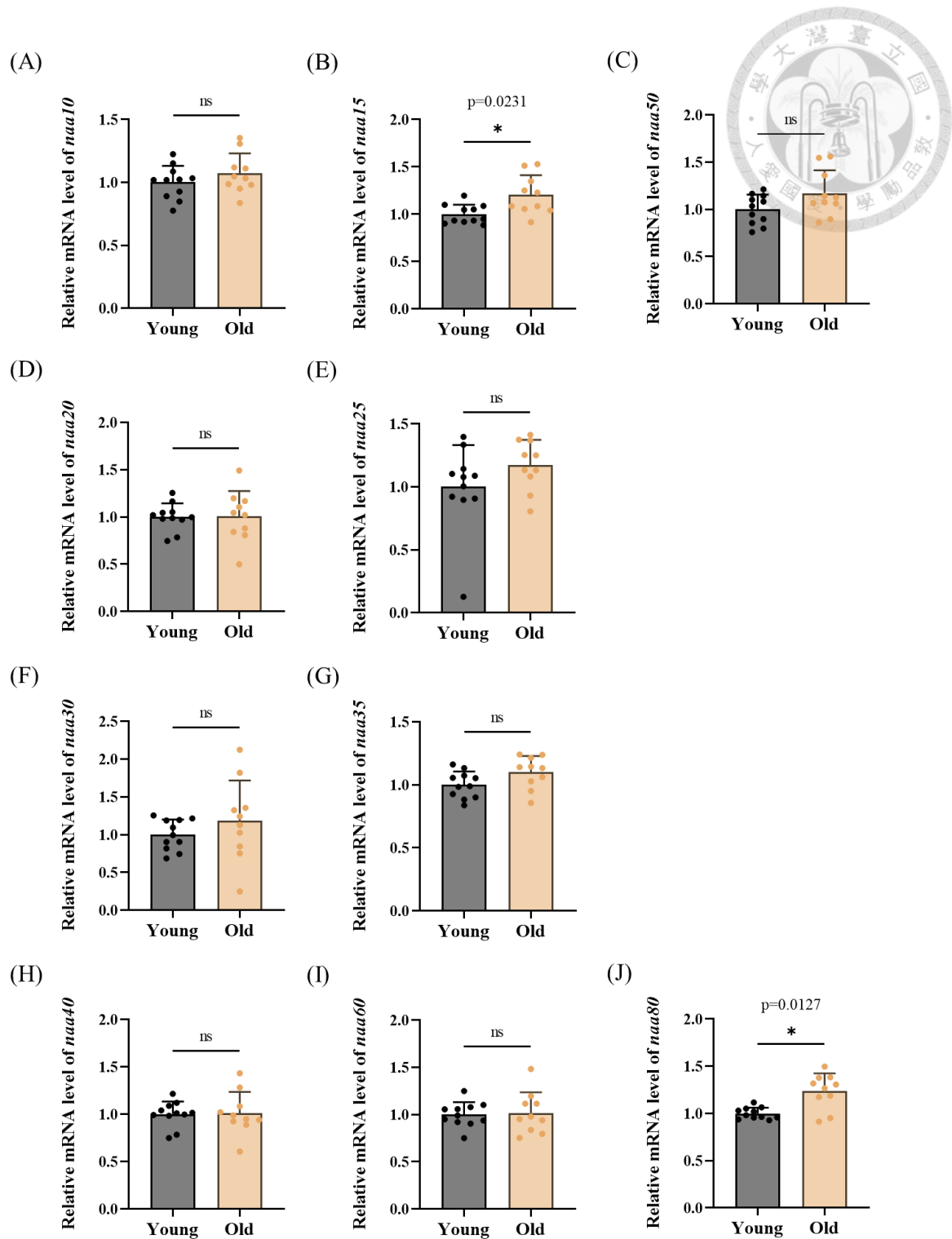
**Figure 11. mRNA levels of *Naa15* and *Naa80* are significantly higher in the SVZ of aged mice.**

RT-qPCR analysis was used to investigate the mRNA levels of 10 Nat genes in SVZ tissue of young (2-3 mo., n=11) and old mice (19-20 mo., n=12). The $2^{-\Delta\Delta CT}$ method was

employed to assess the relative mRNA levels by normalizing them to *gapdh* expression and then expressing them relative to the levels in young mice. Error bars represent the standard deviations.
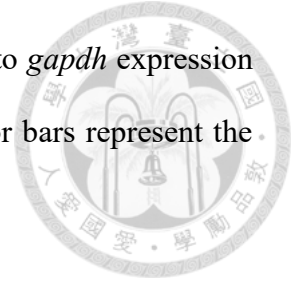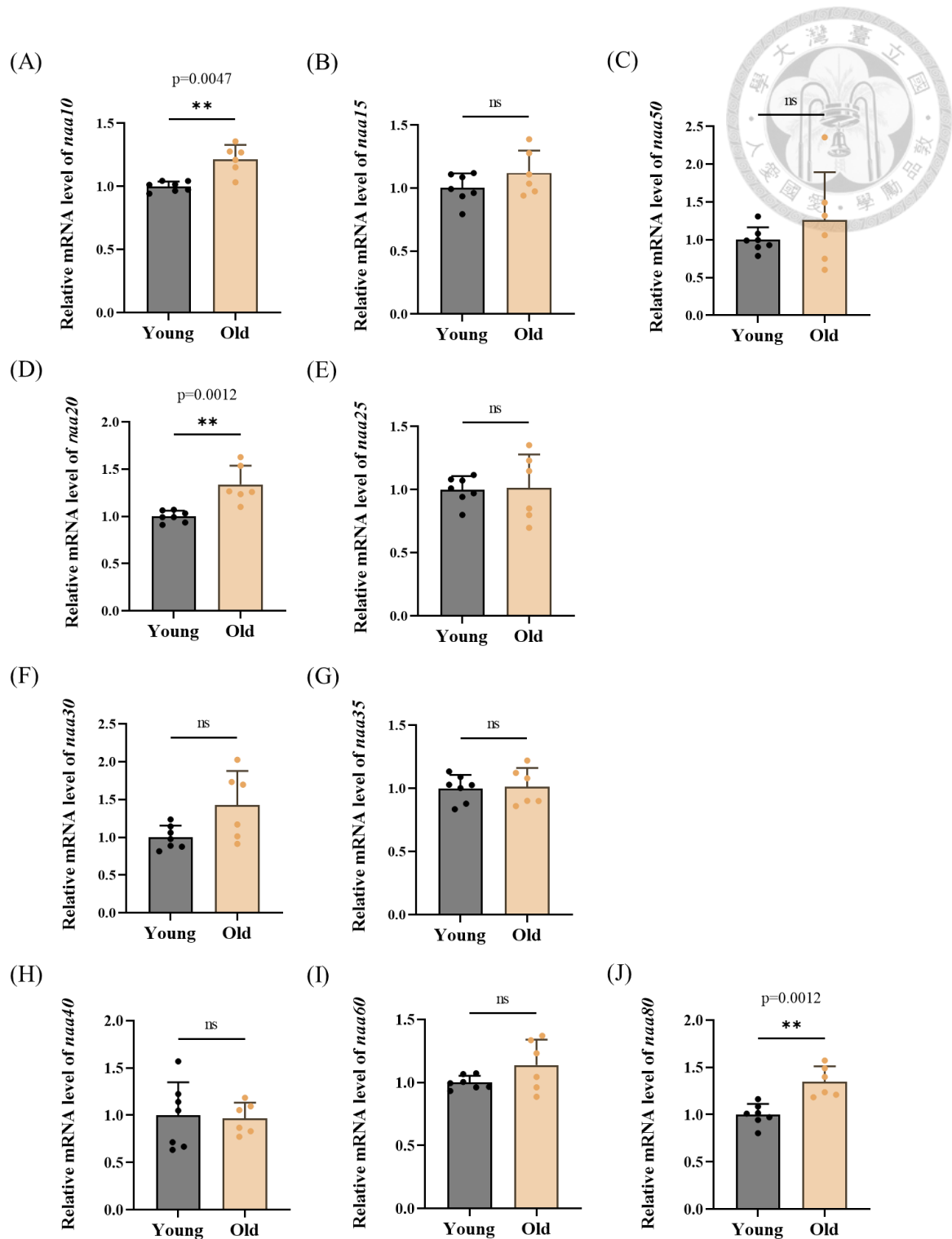
Figure 12. mRNA levels of *Naa10*, *Naa20* and *Naa80* are significantly higher in the DG of aged mice.

RT-qPCR analysis was performed to examine the mRNA levels of 10 NAT genes in SVZ tissue of young (2-3 mo., n=7) and old mice (19-20 mo., n=6). The $2^{-\Delta\Delta CT}$ method was

employed to assess the relative mRNA levels by normalizing them to *gapdh* expression

and then expressing them relative to the levels in young mice. Error bars represent the

standard deviations.
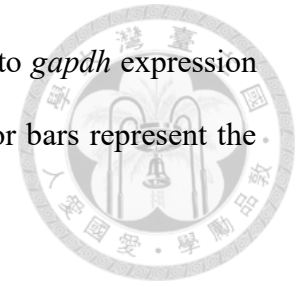
3. Discussion

3.1. Neurosphere culture medium screening
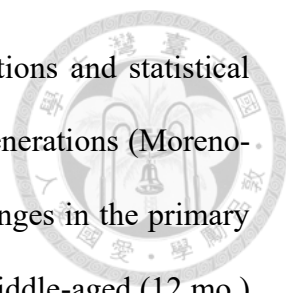
Our study conducted the first comprehensive comparison of the efficiency of the widely used NSC neurosphere culture medium. Building upon existing formulations, we also explored new formulas, including a series derived from NSCBM (M7, M9, M13-21). Taking into consideration the maximal formation and the highest neurosphere-forming capability, along with cost factors, we ultimately selected M12 (a combination of DMEM-F12 and NB in a 1:1 ratio was mixed with a 1:1 combination of N2 and B27) as the neurosphere culture medium. This medium was employed for the rapid visualization of neuronal differentiation in neurospheres (Lee et al., 2020) and the differentiation of adult SVZ-derived aNS-1 cells (Goffredo et al., 2008).

Additionally, among the five mediums capable of forming neurospheres (M6, M11, M12, M14, M21), three have never been reported before (M11, M14, M21). Hence, our study successfully tested the availability of these three neurosphere culture mediums for the first time.

3.2. Neurosphere forming capacity

The question of whether aging SVZ cells form fewer neurospheres has been a subject of ongoing debate. Given that neurogenesis ability in the adult brain declines with aging, consistent with this notion, research has revealed a significant decrease in the yield of primary neurospheres obtained from aged SVZ (22–26 mo.) compared to young mice (3-5 mo.). However, after multiple passages, this decline in the neurosphere-forming ability of aging neurospheres is no longer evident (Ahlenius et al., 2009).

Likewise, certain research has suggested a decline in the number of neurospheres in aged mice (24 months old) in comparison to their younger counterparts (2 months old),
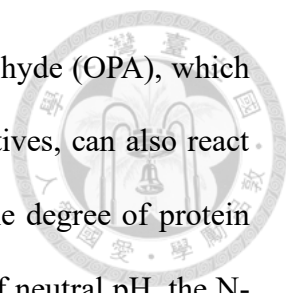
but these studies did not explicitly specify the neurosphere generations and statistical methods used, nor did they compare differences between different generations (Moreno-Cugnon et al., 2020). In contrast, other researchers observed no changes in the primary and P1 neurosphere-forming capacity of SVZ neural precursors in middle-aged (12 mo.) and young mice (2 mo.) (Bouab et al., 2011). These contradictory findings underscore the complexity within the research field and highlight the unique contribution of our study.

It is worth noting that our improved culture system provides an effective model for studying the aging of NSCs. So far, there is no medium available that can sustain the difference in NSCs from young and old individuals. Our system allows the observation of the age-dependent decline in neurosphere formation capacity. The divergence between our study and previous research may stem from multiple factors, with a key element being the utilization of our modified culture system, enabling a more effective observation of the aging characteristics of neural stem cells. In contrast, other studies may have employed different culture conditions or methods, leading to disparate results. This emphasizes the uniqueness of our research and its contribution to a more comprehensive understanding of the mechanisms underlying the aging of neurogenesis capabilities.

3.3. Protein N-terminal acetylation

3.3.1. Cultured SVZ-NSCs and SVZ tissue

Traditional methods for analyzing N-terminal acetylation often involve enriching N-terminal peptides and characterizing them through mass spectrometry. Therefore, we utilized the NBD-Cl assay, a direct and sensitive fluorescence-based technique, to distinguish the unbound N-termini. The NBD-Cl assay relies on the emission of fluorescence upon the binding of NBD to the protein's free N-terminal residue. Concerns may arise about potential interference with fluorescence due to the interaction between

NBD-Cl and lysine. Indeed, fluorogenic reagents like o-phthaldialdehyde (OPA), which reacts with primary amines to generate fluorescent isoindole derivatives, can also react with lysine side chains and thereby hinder the ability to measure the degree of protein NAc. However, according to Bernal-Perez et al., Under conditions of neutral pH, the N-termini selectively undergoes a reaction with NBD–Cl, whereas the amino groups in the side chain of lysine remain unresponsive (Bernal-Perez et al., 2012). Thus, NBD-Cl proves to be a robust method for distinguishing protein N-terminal. Using this method, we observed a decreased free N-terminal level of proteins in aged cultured SVZ-NSCs. Consistently, we observed the same changes in aged SVZ tissue, suggesting that the aging mechanism of SVZ NSCs could be associated with the downregulation of free N-termini.

Although a decrease in protein-free N-terminal level, suggesting an increase in protein N-terminal acetylation, is observed in both aged cultured SVZ-NSCs and SVZ tissue, the proteins they regulate may differ. In cultured SVZ-NSCs, we found increased mRNA expressions of *naa25* and *naa35*, while in SVZ tissue, *naa15* and *naa80* were found to increase. *naa25*, *naa35*, *naa15*, and *naa80* belong to different NAT families, thus acetylating distinct substrates. This difference may be attributed to the highly heterogeneous environment of SVZ tissue, while in the culture system, NSCs are enriched after passaging. Therefore, in the SVZ, NSCs and other cells in the microenvironment may regulate aging through the N-terminal acetylation of different proteins.

It is noteworthy that, besides NAT expression, other factors may contribute to protein N-terminal acetylation. The increase in acetylation might stem from substrate recruitment, while factors such as acetyl-CoA availability and the interplay between pathways could also play a role. Apart from substrate recruitment, alterations in acetyltransferase and deacetylase activity may contribute to heightened acetylation.

3.3.2. SVZ and DG

In contrast to SVZ tissue, there is no alteration observed in protein free N-terminal level in aged mice. NSCs from the DG and SVZ are situated in different anatomical locations and exhibit distinct functionalities. Neurons originating from NSCs in the adult DG are excitatory, whereas SVZ-NSCs give rise to inhibitory neurons. DG-NSCs also demonstrate the ability to generate differentiated astrocytes, yet they do not appear to produce oligodendrocytes under normal conditions (Obernier & Alvarez-Buylla, 2019). Therefore, the distinct aging regulatory mechanisms in the DG and SVZ appears plausible. Despite there being no alteration in protein N-terminal acetylation in the aged DG, the mRNA levels of *naa10*, *naa20*, and *naa80* increase. This suggests that protein N-terminal acetylation in the DG may still be involved in the aging regulatory pathway. Further exploration is necessary to unravel these interactions and identify specific reasons for acetylation changes during the aging process.

4. Conclusion

In summary, our research successfully established an adult neurosphere culture system, revealing age-related variations in NSC forming ability. We confirmed the presence of NSCs in both young and aged neurospheres, showcasing their proliferative and differentiation capabilities. Notably, the culture system highlighted a significant decline in neurosphere-forming and proliferative abilities in aged NSCs, persisting through multiple passages, establishing it as a robust model for studying neurogenesis aging.

Our study delved into the role of protein NAc in NSC aging, revealing an increased NAc ratio for TMSB10, PPIA, SLC6A11, and PSMD1, and a decreased NAc ratio for DDT. Additionally, we observed downregulated levels of free N-terminal level in aged neurospheres, suggesting that global N-terminal acetylation is increased during aging. Interestingly, the free N-terminal level displayed tissue-specific patterns in different brain regions. These findings enhance our understanding of the regulatory mechanisms governing adult neurogenesis and provide valuable insights into the aging process of NSCs.

5. Materials and Methods

5.1. Mice
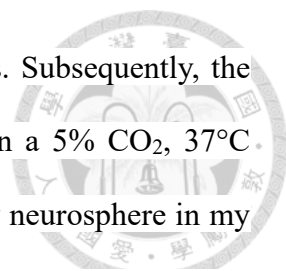
SPF inbred C57BL/6JNarl mice were obtained from the National Laboratory Animal Center (NLAC), NARLabs, Taiwan. This study utilized young (2-4 mo.) and old (19-20 mo.) female adult mice. The mice were housed in the Academia Sinica SPF animal facility, and all animal-related protocols were carried out in compliance with the guidelines and approvals of the Institutional Animal Care and Use Committee (IACUC).

5.2. Tissue dissociation

Surgically remove the mouse brain and transfer it to ice-cold dissection buffer (1x Hank's balanced salt solution containing 2 mM HEPES and primocin). To obtain coronal slices, make a cut along the optic nerve of the mouse brain. The SVZ tissue was microdissected from coronal slices of mouse brains following the protocols by Ahmed et al., 2021. For the remaining posterior part of the mouse brain, divide it into equal halves along the sagittal plane and obtain DG following the methods described by Hagihara et al., 2009. Mince SVZ or DG with fine scissors and quickly mix them with 10 mL of ice-cold dissection buffer separately. Finally, spin down the tissue at 200 g for 5 minutes at 18°C–25°C for subsequent protein extraction or cell culture.

5.3. Neurosphere culture

The prepared SVZ tissue was subjected to digestion with 1 ml of accutase, and the reaction was allowed to proceed at room temperature for 30 minutes, with gentle pipetting every 15 minutes (20 times). Following this, 5 ml of wash medium was added and thoroughly mixed. The mixture was then centrifuged at 300 g for 5 minutes, and this process was repeated twice. The cells were resuspended in 1 ml of growth media and

passed through a 100 μm cell strainer to eliminate undigested cells. Subsequently, the cells were seeded onto an ultra-low 24-well plate and incubated in a 5% CO_2, 37°C environment for 7 days. This stage is identified as P0 or the primary neurosphere in my study. After 7 days, the P0 neurospheres were harvested and transferred to an ultra-low 6-well plate, with the volume adjusted to 3 ml using growth media. The plate was then incubated in a 5% CO_2, 37°C environment for an additional 7 days, marking this stage as P1 neurosphere. Thereafter, every 7 days, the neurospheres were subjected to a 1 ml accutase digestion for passaging and continued cultivation.

5.4. Neurosphere-forming capacity

In this study, we employed P0-P3 neurospheres to assess their neurosphere-forming capacity. After culturing each generation of neurospheres for 7 days, they were individually collected, digested with accutase, and then counted following filtration through a 100 μm cell strainer. The counting procedure involved the addition of trypan blue to distinguish between live and dead cells. Subsequently, 10,000 live cells were seeded in each well of ultra-low 96-well plates, with each sample subjected to triplicate testing. After 7 days, photographs were taken using a microscope, and the number and diameter of neurospheres were measured using ImageJ 1.54f.

5.5. Immunofluorescence

24-well plates were coated with poly-L-ornithine (PLO) for 1 hour at 37°C, followed by three washes with PBS. Subsequently, the plates were coated with laminin for 3 hours at 37°C or overnight at 4°C. The coated plates could be stored long-term at 4°C for later use. Neurospheres were digested using accutase for 10 minutes at room temperature and

then cultured in a monolayer on PLO-laminin-coated 24-well plates. The initial cell seeding density was 50,000 cells per well in growth medium.

For NSC staining, cells were fixed the following day. In the NSC differentiation assay, cells were grown in growth medium for 1 day and then switched to differentiation medium (growth medium without the growth factors EGF and FGF) for 3 days. Cells were washed twice with PBS and fixed in 4% paraformaldehyde (PFA) for 30 minutes at room temperature, permeabilized with 0.1% Triton X-100 in PBS for 15 minutes, and blocked in 3% BSA in 0.01% Triton X-100 in PBS for 30 minutes at room temperature.

Primary antibodies were diluted in 3% BSA in 0.01% Triton X-100 in PBS and incubated at 4°C overnight. The primary antibodies used in these experiments were Nestin (Merck Millipore; 1:50), Vimentin (Proteintech, 1:500), Gfap (Sigma, 1:50), Sox2 (Proteintech, 1:50), Tuj1 (GeneTex, 1:100). Subsequently, cells were washed three times with PBS and incubated with secondary antibodies (anti-mouse-FITC, 1:500, or anti-rabbit-TexRed, 1:500) for 1 hour at room temperature. Plates were washed three times with PBS, and cell nuclei were stained with DAPI. Images were acquired using an ImageXpress Confocal HT.ai.

5.6. Cell proliferation and cell survival rate

Following the same procedure as for assessing neurosphere-forming capacity, after culturing the cells in 96-well plates for 7 days and capturing images, the cells were gathered, digested with 1 ml of accutase, washed twice with 5 ml of wash medium, and then suspended in 1 ml of growth media. Subsequently, the cells were filtered through a 100 μm cell strainer, and trypan blue stain was used for cell counting. Dead cells were stained blue, while live cells remained unstained. Cell proliferation was calculated as the

ratio of the total cell number to the initial cell count, whereas the cell survival rate was determined by calculating the proportion of dead cells relative to the total cell number.
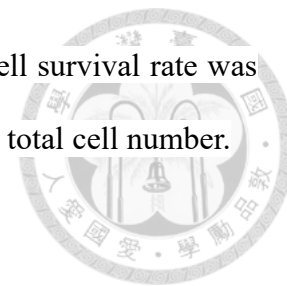
5.7. NBD-Cl assay

A stock solution of 50 mM NBD-Cl was prepared in 50 mM citrate buffer (pH 7.0) with 1 mM EDTA and stored at 4°C in the dark. For SVZ and DG tissue, the tissue was digested with 1 ml of trypsin at 37°C for 15 minutes, and then 10 ml of trypsin inhibitor was added. The mixture was centrifuged, and the supernatant was removed. After that, 300 µl of citrate lysis buffer was added. For neurospheres, 300 µl of citrate lysis buffer was directly added. Subsequently, a 27 G needle was used to aspirate the solution multiple times to break down the cells. The sample was then centrifuged at 14,000 g for 15 minutes to remove undissolved cell debris. The supernatant was transferred to a clean tube, and the protein concentration was measured using the Bradford assay. Ten micrograms of protein were serially diluted and mixed with 0.5 mM NBD in 50 mM citrate buffer (pH 7.0) with 1 mM EDTA. The reaction was carried out at room temperature in the dark overnight. After the reaction was completed, fluorescence was measured using an ELISA, and the fluorescence values for each unit of protein were calculated.

5.8. RNA isolation and reverse transcriptase-PCR.

For RNA isolation, tissues or neurospheres were centrifuged and then lysed with RLT buffer. Total RNA was extracted using the RNeasy Plus Mini Kit. Subsequently, the RNA concentration was quantified using a Nanodrop spectrophotometer. To synthesize cDNA, less than 5 µg of total RNA was used, along with dNTPs and an oligo-dT primer. The reaction started with incubation at 65°C for 5 minutes, followed by cooling to 2°C on ice. Afterward, DTT, SS4 enzyme, and 5x buffer were added, and the reaction was carried out:

first at 65°C for 5 minutes, then at 53°C for 10 minutes, and finally at 80°C for 10 minutes, completing the cDNA conversion process.

To quantitatively analyze the mRNAs of Nat genes, real-time PCR was conducted on a LightCycler 480 using SYBR Green. The PCR amplification included the following parameters: initial denaturation at 95°C for 5 minutes, followed by 40 cycles of denaturation at 95°C for 10 seconds, annealing at 55°C for 20 seconds, and extension at 72°C for 30 seconds. Each primer set exhibited a single peak in the melting curve analysis, confirming the absence of false signals. Gapdh served as an internal control to normalize the mRNA levels. The specific oligonucleotide primer sets utilized in this study are listed in Table 4.

Table 4. Primers for RT-qPCR.

Name	Direction	Sequence (5' to 3')
gapdh	Forward	CATCACTGCCACCCAGAAGACTG
gapdh	Reverse	ATGCCAGTGAGCTTCCCGTTCAG
mNaa10	Forward	ACCTCACGCAGATGGCTGATGA
mNaa10	Reverse	GCTCAGAAGCACGTTGCCTTTG
mNaa15	Forward	TGGTCAGCCATCCATTGCTCTG
mNaa15	Reverse	CCATCCACCTGGCAGCTTCTTT
mNaa20	Forward	TTCATCGTCGCTGAAGCACCTG
mNaa20	Reverse	GTCCATGCCATTCTTCCCTAGC
mNaa25	Forward	TACTGCCTGCTCGCTGTTCATG
mNaa25	Reverse	AGCCTTCTTCCAGCAGAGTCAG
mNaa30	Forward	TGCCATGGTTGAAGGAGACTGTG
mNaa30	Reverse	CAGCCTCTTATCTCGAACAAAACC
mNaa35	Forward	CTGCTCACAGTGCTCATAGCCT
mNaa35	Reverse	TGGTAGTGCCATTCTGAGCCTG
mNaa50	Forward	CCAGGTCATCTTTCCAGTCAGC
mNaa50	Reverse	ATGATCCACCCTGCAGCACACT
mNaa60	Forward	TGAAGCACCTGTGTGGCGACTG
mNaa60	Reverse	CCACAATGGCACCTCTGTAGGT
mNaa80	Forward	CTCAACACCAGGCAAAGGAGCT
mNaa80	Reverse	GAGATCAGCACAGGCACTCATG

50
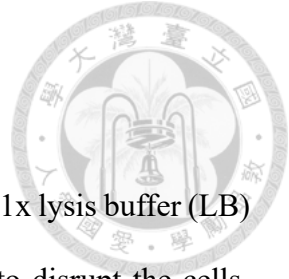
5.9. Analysis of protein NAc by LC-MS/MS

5.9.1. Protein extraction for proteomics
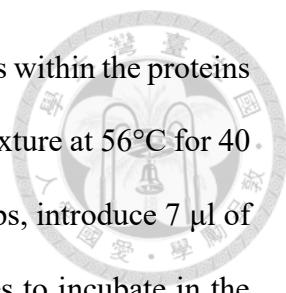
Tissues or neurospheres were centrifuged to form a pellet. Then, 1x lysis buffer (LB) was added, followed by vigorous pipetting up and down 10 times to disrupt the cells. Afterward, the sample was centrifuged, and ultrasonic vibration was performed for 15 minutes (30 seconds on/30 seconds off). Finally, the mixture was boiled at 95°C for 5 minutes.

5.9.2. Removal of the detergents

To remove detergents in the protein samples, begin by adding 0.4 ml of methanol to 0.1 ml of the protein sample and vortex the mixture thoroughly. Centrifuge the samples at 9000g for 10 seconds to collect the entire sample. Next, introduce 0.1 ml of chloroform to the samples. Vortex the mixture once more and centrifuge again at 9000g for 10 seconds. To facilitate phase separation, add 0.3 ml of water. Vigorously vortex the samples and centrifuge for 1 minute at 9000g. Carefully remove and discard the upper phase. Now, add an additional 0.3 ml of methanol to the remaining lower chloroform phase and the interphase that contains the precipitated protein. Mix the samples and centrifuge again for 2 minutes at 9000g to pellet the protein. Finally, remove the supernatant and dry the protein pellet using a stream of air. The dried pellet is now ready for storage until further use.

5.9.3. Protein reduction and alkylation

Reconstitute the precipitated proteins in a 50 mM NH_4HCO_3 solution to achieve a concentration of 1 µg/µl. Incubate the mixture at 25°C for 1 hour in a thermomixer operating at 600 rpm (alternatively, consider using vortexing or sonication for better

dissolution). For a 15 µl sample, thoroughly reduce the disulfide bonds within the proteins by adding 2 µl of 85 mM DTT in 50 mM NH_4HCO_3. Incubate this mixture at 56°C for 40 minutes, maintaining agitation at 600 rpm. To alkylate the thiol groups, introduce 7 µl of 55 mM IAA in 50 mM NH_4HCO_3 to the samples. Allow the samples to incubate in the dark at 25°C for 30 minutes with continuous agitation at 600 rpm. Any remaining unreacted IAA can be neutralized by adding 3 µl of 85 mM DTT in 50 mM NH_4HCO_3 and incubating in the dark at 25°C for 10 minutes at 600 rpm.

5.9.4. Protein Digestion

Conduct an in-solution digestion at 37°C overnight, using a trypsin-to-sample ratio of 1:50 (w/w). Halt the digestion by rapidly freezing the mixture at -80°C. Subsequently, use a speed-vac to vacuum-dry the tryptic peptide mixtures, and then store them safely at -20°C until they are ready for proteome analysis.

5.9.5. High pH reversed-phase peptide fractionation

The experiment was carried out following the guidelines provided in the Pierce High pH Reversed-Phase Peptide Fractionation Kit Instructions. Before starting, it is essential to condition the Spin Columns properly. Begin by removing the protective white tip from the bottom of the column and disposing of it. Insert the column into a 2.0 mL sample tube (if using a 1.5 mL tube, ensure that the flow-through contacts the bottom of the column). Centrifuge at 5000 × g for 2 minutes to eliminate the solution and compact the resin material. Discard the liquid. Next, remove the top screw cap and introduce 300 µL of acetonitrile (ACN) into the column. Replace the cap, position the spin column back into a 2.0 mL sample tube, and centrifuge at 5000 × g for 2 minutes. Discard the ACN and

repeat this washing step. Wash the spin column twice with a 0.1% trifluoroacetic acid (TFA) solution. The column is now conditioned and prepared for use.

Following the conditioning of the Spin Columns, the process of fractionating digest samples can commence. Prepare elution solutions in accordance with the specifications provided in Table 5. Start by dissolving 10-100 μg of the digested sample in 300 μL of a 0.1% TFA solution. It is essential to ensure that peptide samples are completely dissolved and free from any organic solvents (e.g., ACN, DMSO, etc.). Place the spin column into a fresh 2.0 mL sample tube. Load 300 μL of the sample solution onto the column, then replace the top cap and centrifuge at 3000 × g for 2 minutes. Retain the eluate as the 'flow-through' fraction. Subsequently, position the column into another 2.0 mL sample tube. Load 300 μL of water onto the column and centrifuge again to collect the wash. Keep the eluate as the 'wash' fraction. Place the column into a new 2.0 mL sample tube. Load 300 μL of the appropriate elution solution (e.g., 5% ACN, 0.1% TEA) and centrifuge at 3000 × g for 2 minutes to collect the fraction. Repeat this step for the remaining step gradient fractions, utilizing the suitable elution solutions outlined in Table 5 and using new 2.0 mL sample tubes. Finally, evaporate the liquid contents of each sample tube to dryness using vacuum centrifugation, such as a SpeedVac concentrator. The samples are now ready for analysis by LC-MS/MS.

MS raw data were got from Mass core of GRC and were processed by Chein-Hung Chen using Mascot and mouse protein database from UniProt for MS/MS ion search. The mass tolerance of precursor and fragment ions was set at 8 ppm and 0.1 Da, respectively. Carbamidomethyl on Cys was fixed modification, acetyl on protein N-terminal, oxidation on Met and deamidated on Asn and Gln were specified as the variable modification for amino acids. Trypsin was designated as the digestion enzyme with allowance for up to 2 missed cleavages.

Table 5. Preparation of elution solutions for unlabeled, native peptides.

Fraction No.	Acetonitrile (%)	Acetonitrile (µL)	Triethylamine (0.1%) (µL)
1	5.0	50	950
2	7.5	75	925
3	10.0	100	900
4	12.5	125	875
5	15.0	150	850
6	17.5	175	825
7	20.0	200	800
8	50.0	500	500

5.10. Data analysis
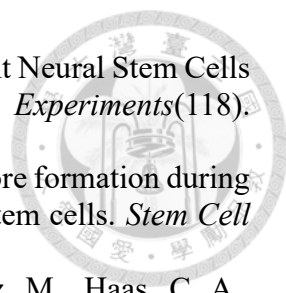
All experiments were independently replicated, and the results were presented as means with standard deviation (SD). For neurosphere-forming capacity, cell proliferation, cell survival rate, NBD-Cl assay and RT-qPCR, statistical significance was determined using Mann Whitney test and assessed using GraphPad Prism (version 9.5.0). A P-value <0.05 was deemed statistically significant. For the analysis of protein NAc by LC-MS/MS, the data were first normalized using Progenesis QI to calculate normalized abundance based on MS1 intensity, utilizing label-free quantification methods by the GRC MS core. Subsequently, the NAc ratio was determined by peptides with NAc/total peptides. Proteins with significantly varied NAc ratios between neurospheres from young and aged mice were identified using a t-test. This study has been revised with the assistance of ChatGPT-3.5.
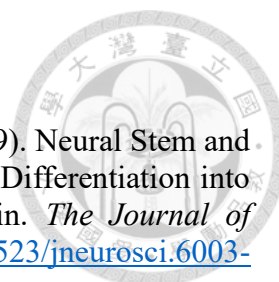
References

Ahlenius, H., Visan, V., Kokaia, M., Lindvall, O., & Kokaia, Z. (2009). Neural Stem and Progenitor Cells Retain Their Potential for Proliferation and Differentiation into Functional Neurons Despite Lower Number in Aged Brain. *The Journal of Neuroscience*, *29*(14), 4408-4419. https://doi.org/10.1523/jneurosci.6003-08.2009

Ahmed, A. K. M. A., Isaksen, T. J., & Yamashita, T. (2021). Protocol Protocol for mouse adult neural stem cell isolation and culture. *Star Protocols*, *2*(2). https://doi.org/ARTN 100522 10.1016/j.xpro.2021.100522

Altman, J., & Das, G. D. (1965). Autoradiographic and Histological Evidence of Postnatal Hippocampal Neurogenesis in Rats. *Journal of Comparative Neurology*, *124*(3), 319-&. https://doi.org/DOI 10.1002/cne.901240303

Angata, K., & Fukuda, M. (2010). Roles of Polysialic Acid in Migration and Differentiation of Neural Stem Cells. *Methods in Enzymology, Vol 479: Functional Glycomics*, *479*, 25-36. https://doi.org/10.1016/S0076-6879(10)79002-9

Apostolopoulou, M., Kiehl, T. R., Winter, M., Cardenas De La Hoz, E., Boles, N. C., Bjornsson, C. S., Zuloaga, K. L., Goderie, S. K., Wang, Y., Cohen, A. R., & Temple, S. (2017). Non-monotonic Changes in Progenitor Cell Behavior and Gene Expression during Aging of the Adult V-SVZ Neural Stem Cell Niche. *Stem Cell Reports*, *9*(6), 1931-1947. https://doi.org/10.1016/j.stemcr.2017.10.005

Audesse, A. J., & Webb, A. E. (2018). Enhancing Lysosomal Activation Restores Neural Stem Cell Function During Aging. *Journal of Experimental Neuroscience*, *12*, 117906951879587. https://doi.org/10.1177/1179069518795874

Audesse, A. J., & Webb, A. E. (2020). Mechanisms of enhanced quiescence in neural stem cell aging. *Mechanisms of Ageing and Development*, *191*, 111323. https://doi.org/10.1016/j.mad.2020.111323

Bernal-Perez, L. F., Prokai, L., & Ryu, Y. (2012). Selective N-terminal fluorescent labeling of proteins using 4-chloro-7-nitrobenzofurazan: a method to distinguish protein N-terminal acetylation. *Anal Biochem*, *428*(1), 13-15. https://doi.org/10.1016/j.ab.2012.05.026

Bond, A. M., Ming, G. L., & Song, H. (2015). Adult Mammalian Neural Stem Cells and Neurogenesis: Five Decades Later. *Cell Stem Cell*, *17*(4), 385-395. https://doi.org/10.1016/j.stem.2015.09.003

Bouab, M., Paliouras, G. N., Aumont, A., Forest-Bérard, K., & Fernandes, K. J. L. (2011). Aging of the Subventricular Zone Neural Stem Cell Niche: Evidence for Quiescence-Associated Changes between Early and Mid-Adulthood. *Neuroscience*, *173*, 135-149. https://doi.org/10.1016/j.neuroscience.2010.11.032

Bragado Alonso, S., Reinert, J. K., Marichal, N., Massalini, S., Berninger, B., Kuner, T., & Calegari, F. (2019). An increase in neural stem cells and olfactory bulb adult neurogenesis improves discrimination of highly similar odorants. *EMBO J*, *38*(6). https://doi.org/10.15252/embj.201798791

Breton-Provencher, V., Lemasson, M., Peralta, M. R., 3rd, & Saghatelyan, A. (2009). Interneurons produced in adulthood are required for the normal functioning of the olfactory bulb network and for the execution of selected olfactory behaviors. *J Neurosci*, *29*(48), 15245-15257. https://doi.org/10.1523/JNEUROSCI.3606-09.2009

Cutler, R. R., & Kokovay, E. (2020). Rejuvenating subventricular zone neurogenesis in

the aging brain. *Curr Opin Pharmacol*, *50*, 1-8. https://doi.org/10.1016/j.coph.2019.10.005

Dissmeyer, N., Graciet, E., Holdsworth, M. J., & Gibbs, D. J. (2019). N-term 2017: Proteostasis via the N-terminus. *Trends Biochem Sci*, *44*(4), 293-295. https://doi.org/10.1016/j.tibs.2017.11.006

Donato, R., Miljan, E. A., Hines, S. J., Aouabdi, S., Pollock, K., Patel, S., Edwards, F. A., & Sinden, J. D. (2007). Differential development of neuronal physiological responsiveness in two human neural stem cell lines. *BMC Neuroscience*, *8*(1), 36. https://doi.org/10.1186/1471-2202-8-36

Esteve, D., Molina-Navarro, M. M., Giraldo, E., Martínez-Varea, N., Blanco-Gandia, M.-C., Rodríguez-Arias, M., García-Verdugo, J. M., Viña, J., & Lloret, A. (2022). Adult Neural Stem Cell Migration Is Impaired in a Mouse Model of Alzheimer's Disease. *Molecular Neurobiology*, *59*(2), 1168-1182. https://doi.org/10.1007/s12035-021-02620-6

Goffredo, D., Conti, L., Di Febo, F., Biella, G., Tosoni, A., Vago, G., Biunno, I., Moiana, A., Bolognini, D., Toselli, M., & Cattaneo, E. (2008). Setting the conditions for efficient, robust and reproducible generation of functionally active neurons from adult subventricular zone-derived neural stem cells. *Cell Death & Differentiation*, *15*(12), 1847-1856. https://doi.org/10.1038/cdd.2008.118

Hagihara, H., Toyama, K., Yamasaki, N., & Miyakawa, T. (2009). Dissection of hippocampal dentate gyrus from adult mouse. *J Vis Exp*(33). https://doi.org/10.3791/1543

Hou, Y. J., Dan, X. L., Babbar, M., Wei, Y., Hasselbalch, S. G., Croteau, D. L., & Bohr, V. A. (2019). Ageing as a risk factor for neurodegenerative disease. *Nature Reviews Neurology*, *15*(10), 565-581. https://doi.org/10.1038/s41582-019-0244-7

Ibrayeva, A., Bay, M., Pu, E., Jörg, D. J., Peng, L., Jun, H., Zhang, N., Aaron, D., Lin, C., Resler, G., Hidalgo, A., Jang, M.-H., Simons, B. D., & Bonaguidi, M. A. (2021). Early stem cell aging in the mature brain. *Cell Stem Cell*, *28*(5), 955-966.e957. https://doi.org/10.1016/j.stem.2021.03.018

Juan, Tatyana, Peunova, N., Park, J.-H., Tordo, J., Daniel, Fishell, G., Koulakov, A., & Enikolopov, G. (2011). Division-Coupled Astrocytic Differentiation and Age-Related Depletion of Neural Stem Cells in the Adult Hippocampus. *Cell Stem Cell*, *8*(5), 566-579. https://doi.org/10.1016/j.stem.2011.03.010

Kaise, T., Fukui, M., Sueda, R., Piao, W., Yamada, M., Kobayashi, T., Imayoshi, I., & Kageyama, R. (2022). Functional rejuvenation of aged neural stem cells by Plagl2 and anti-Dyrk1a activity. *Genes & Development*, *36*(1-2), 23-37. https://doi.org/10.1101/gad.349000.121

Kalamakis, G., Brune, D., Ravichandran, S., Bolz, J., Fan, W., Ziebell, F., Stiehl, T., Catala-Martinez, F., Kupke, J., Zhao, S., Llorens-Bobadilla, E., Bauer, K., Limpert, S., Berger, B., Christen, U., Schmezer, P., Mallm, J. P., Berninger, B., Anders, S., . . . Martin-Villalba, A. (2019). Quiescence Modulates Stem Cell Maintenance and Regenerative Capacity in the Aging Brain. *Cell*, *176*(6), 1407-1419 e1414. https://doi.org/10.1016/j.cell.2019.01.040

Kevin Flurkey, J. M. C., D.E. Harrison. (2007). *TThe Mouse in Biomedical Research (Second Edition)* (Vol. Volume III, 2007).

Kim, H. S., Shin, S. M., Kim, S., Nam, Y., Yoo, A., & Moon, M. (2022). Relationship between adult subventricular neurogenesis and Alzheimer's disease: Pathologic roles and therapeutic implications. *Front Aging Neurosci*, *14*, 1002281. https://doi.org/10.3389/fnagi.2022.1002281

Kim, J. Y., Lee, J.-H., & Sun, W. (2016). Isolation and Culture of Adult Neural Stem Cells from the Mouse Subcallosal Zone. *Journal of Visualized Experiments*(118). https://doi.org/10.3791/54929

Lee, J. H., Shaker, M. R., Lee, E., Lee, B., & Sun, W. (2020). NeuroCore formation during differentiation of neurospheres of mouse embryonic neural stem cells. *Stem Cell Res*, *43*, 101691. https://doi.org/10.1016/j.scr.2019.101691

Lugert, S., Basak, O., Knuckles, P., Haussler, U., Fabel, K., Götz, M., Haas, C. A., Kempermann, G., Taylor, V., & Giachino, C. (2010). Quiescent and Active Hippocampal Neural Stem Cells with Distinct Morphologies Respond Selectively to Physiological and Pathological Stimuli and Aging. *Cell Stem Cell*, *6*(5), 445-456. https://doi.org/10.1016/j.stem.2010.03.017

Macnee, W., Rabinovich, R. A., & Choudhury, G. (2014). Ageing and the border between health and disease. *European Respiratory Journal*, *44*(5), 1332-1352. https://doi.org/10.1183/09031936.00134014

Marqués-Torrejón, M. A., Williams, C. A. C., Southgate, B., Alfazema, N., Clements, M. P., Garcia-Diaz, C., Blin, C., Arranz-Emparan, N., Fraser, J., Gammoh, N., Parrinello, S., & Pollard, S. M. (2021). LRIG1 is a gatekeeper to exit from quiescence in adult neural stem cells. *Nature Communications*, *12*(1). https://doi.org/ARTN 2594 10.1038/s41467-021-22813-w

Maslov, A. Y., Barone, T. A., Plunkett, R. J., & Pruitt, S. C. (2004). Neural stem cell detection, characterization, and age-related changes in the subventricular zone of mice. *Journal of Neuroscience*, *24*(7), 1726-1733. https://doi.org/10.1523/Jneurosci.4608-03.2004

Mastroeni, D., Chouliaras, L., Van den Hove, D. L., Nolz, J., Rutten, B. P. F., Delvaux, E., & Coleman, P. D. (2016). Increased 5-hydroxymethylation levels in the sub ventricular zone of the Alzheimer's brain. *Neuroepigenetics*, *6*, 26-31. https://doi.org/10.1016/j.nepig.2016.04.002

McGinn, M. J., Colello, R. J., & Sun, D. (2012). Age-related proteomic changes in the subventricular zone and their association with neural stem/progenitor cell proliferation. *J Neurosci Res*, *90*(6), 1159-1168. https://doi.org/10.1002/jnr.23012

Mich, J. K., Signer, R. A. J., Nakada, D., Pineda, A., Burgess, R. J., Vue, T. Y., Johnson, J. E., & Morrison, S. J. (2014). Prospective identification of functionally distinct stem cells and neurosphere-initiating cells in adult mouse forebrain. *Elife*, *3*. https://doi.org/ARTN e02669 10.7554/eLife.02669

Moreno-Cugnon, L., Arrizabalaga, O., Llarena, I., & Matheu, A. (2020). Elevated p38MAPK activity promotes neural stem cell aging. *Aging*, *12*(7), 6030-6036. https://doi.org/10.18632/aging.102994

Negredo, P. N., Yeo, R. W., & Brunet, A. (2020). Aging and Rejuvenation of Neural Stem Cells and Their Niches. *Cell Stem Cell*, *27*(2), 202-223. https://doi.org/10.1016/j.stem.2020.07.002

Obernier, K., & Alvarez-Buylla, A. (2019). Neural stem cells: origin, heterogeneity and regulation in the adult mammalian brain. *Development*, *146*(4), dev156059. https://doi.org/10.1242/dev.156059

Ree, R., Varland, S., & Arnesen, T. (2018). Spotlight on protein N-terminal acetylation. *Experimental & Molecular Medicine*, *50*(7), 1-13. https://doi.org/10.1038/s12276-018-0116-z

Reynolds, B. A., & Weiss, S. (1992). Generation of Neurons and Astrocytes from Isolated Cells of the Adult Mammalian Central-Nervous-System. *Science*, *255*(5052), 1707-1710. https://doi.org/DOI 10.1126/science.1553558

Richards, L. J., Kilpatrick, T. J., & Bartlett, P. F. (1992). De novo generation of neuronal cells from the adult mouse brain. *Proceedings of the National Academy of Sciences*, *89*(18), 8591-8595. https://doi.org/10.1073/pnas.89.18.8591

Rope, A. F., Wang, K., Evjenth, R., Xing, J. C., Johnston, J. J., Swensen, J. J., Johnson, W. E., Moore, B., Huff, C. D., Bird, L. M., Carey, J. C., Opitz, J. M., Stevens, C. A., Jiang, T., Schank, C., Fain, H. D., Robison, R., Dalley, B., Chin, S., . . . Lyon, G. J. (2011). Using VAAST to Identify an X-Linked Disorder Resulting in Lethality in Male Infants Due to N-Terminal Acetyltransferase Deficiency. *American Journal of Human Genetics*, *89*(1), 28-43. https://doi.org/10.1016/j.ajhg.2011.05.017

Satoh, A., Imai, S. I., & Guarente, L. (2017). The brain, sirtuins, and ageing. *Nat Rev Neurosci*, *18*(6), 362-374. https://doi.org/10.1038/nrn.2017.42

Soares, R., Ribeiro, F. F., Lourenço, D. M., Rodrigues, R. S., Moreira, J. B., Sebastiao, A. M., Morais, V. A., & Xapelli, S. (2021). The neurosphere assay: an effective technique to study neural stem cells. *Neural Regeneration Research*, *16*(11), 2229-2231. https://doi.org/10.4103/1673-5374.310678

Steffen, K. K., MacKay, V. L., Kerr, E. O., Tsuchiya, M., Hu, D., Fox, L. A., Dang, N., Johnston, E. D., Oakes, J. A., Tchao, B. N., Pak, D. N., Fields, S., Kennedy, B. K., & Kaeberlein, M. (2008). Yeast life span extension by depletion of 60S ribosomal subunits is mediated by Gcn4. *Cell*, *133*(2), 292-302. https://doi.org/10.1016/j.cell.2008.02.037

Wachs, F.-P., Couillard-Despres, S., Engelhardt, M., Wilhelm, D., Ploetz, S., Vroemen, M., Kaesbauer, J., Uyanik, G., Klucken, J., Karl, C., Tebbing, J., Svendsen, C., Weidner, N., Kuhn, H.-G., Winkler, J., & Aigner, L. (2003). High Efficacy of Clonal Growth and Expansion of Adult Neural Stem Cells. *Laboratory Investigation*, *83*(7), 949-962. https://doi.org/10.1097/01.lab.0000075556.74231.a5

Walker, T. L., & Kempermann, G. (2014). One Mouse, Two Cultures: Isolation and Culture of Adult Neural Stem Cells from the Two Neurogenic Zones of Individual Mice. *Journal of Visualized Experiments*(84). https://doi.org/10.3791/51225

Wang, X., Dong, C., Sun, L., Zhu, L., Sun, C., Ma, R., Ning, K., Lu, B., Zhang, J., & Xu, J. (2016). Quantitative proteomic analysis of age-related subventricular zone proteins associated with neurodegenerative disease. *Sci Rep*, *6*, 37443. https://doi.org/10.1038/srep37443

Xiao, D., Zhang, W. F., Wang, Q., Li, X., Zhang, Y., Rasouli, J., Casella, G., Ciric, B., Curtis, M., Rostami, A., & Zhang, G. X. (2021). CRISPR-mediated rapid generation of neural cell-specific knockout mice facilitates research in neurophysiology and pathology. *Molecular Therapy-Methods & Clinical Development*, *20*, 755-764. https://doi.org/10.1016/j.omtm.2021.02.012
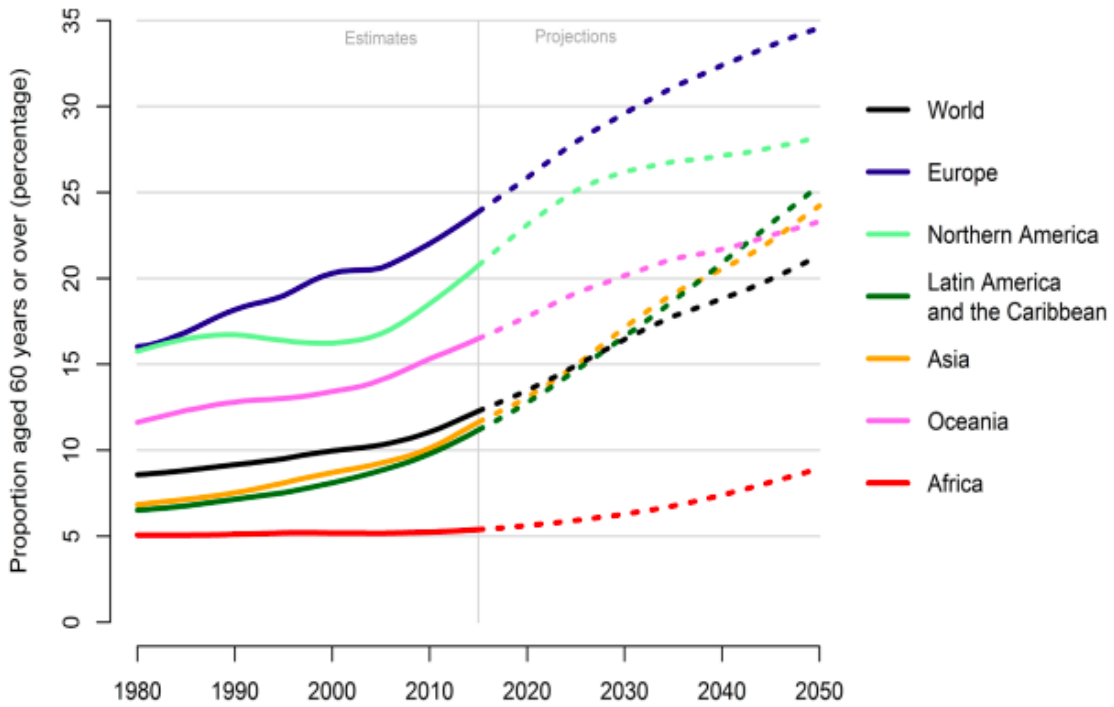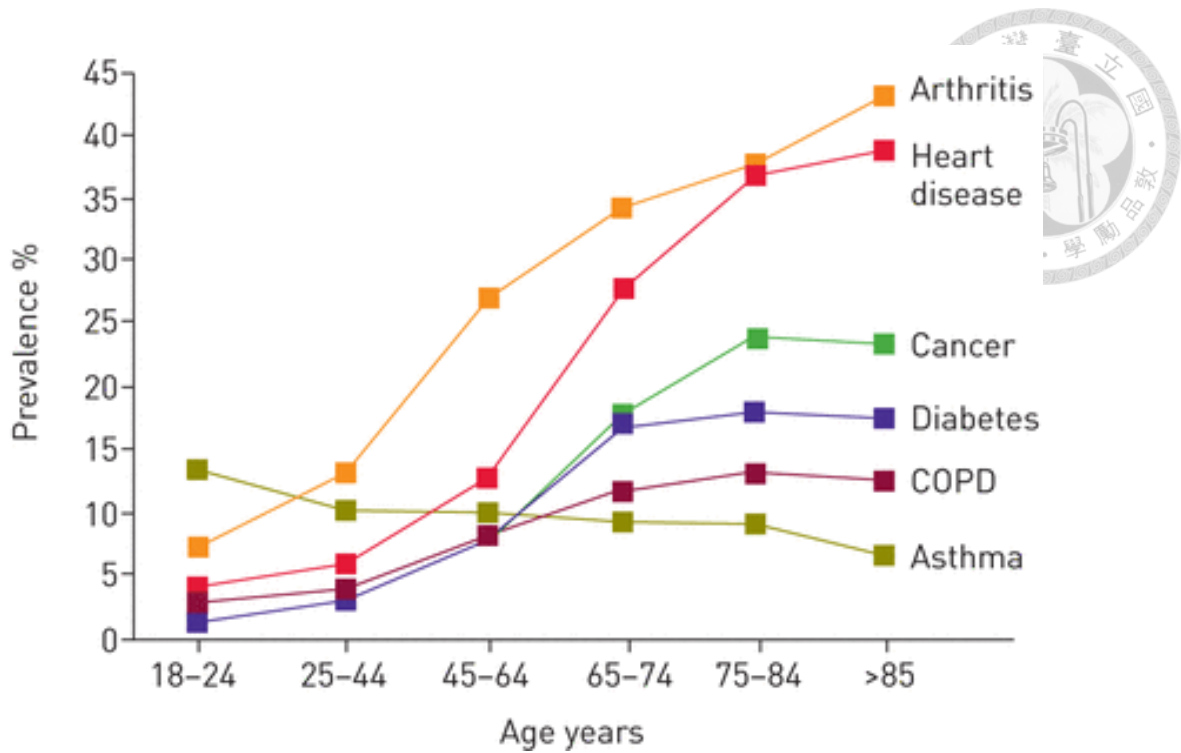
Appendix

Appendix 1. The global elderly population is experiencing rapid and continuous growth.

Percentage of individuals aged 60 years or more by region, spanning from 1980 to 2050.

Source: United Nations, World Population Prospects. The 2017 Revision.
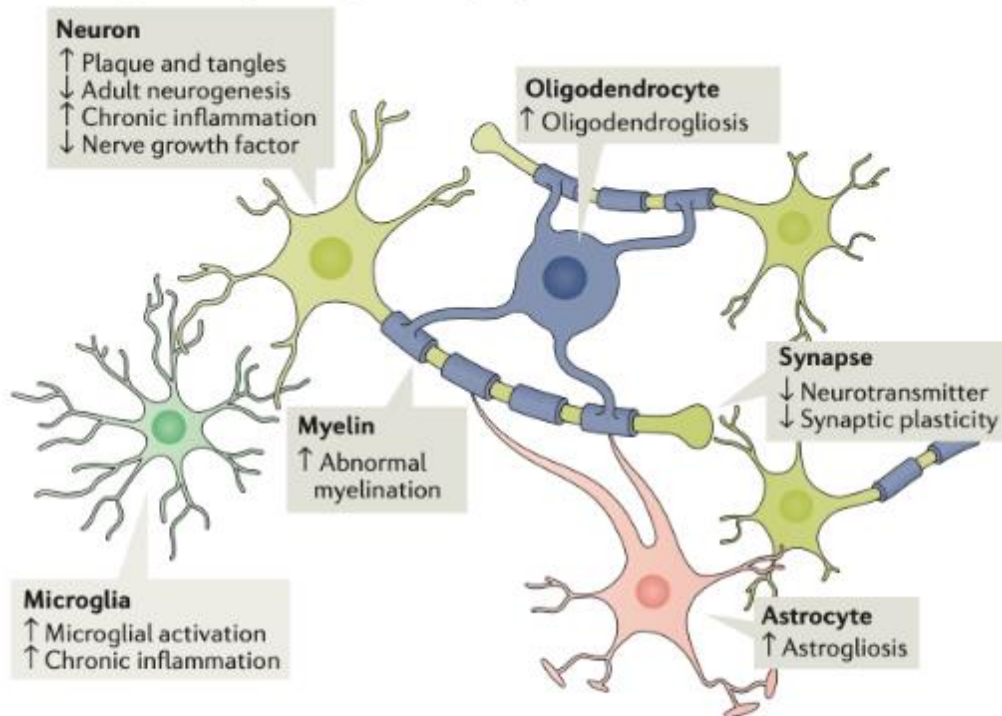
Appendix 2. The prevalence of various chronic diseases increases with age (taken from Macnee et al., 2014).

The chart depicts the prevalence of specific chronic conditions in correlation with age. COPD: chronic obstructive pulmonary disease. MacNee and Rabinovich, Choudhury, 2014, The European respiratory journal, 44(5), 1332–1352.

a Histological changes during normal ageing

Neuron
↑ Plaque and tangles
↓ Adult neurogenesis
↑ Chronic inflammation
↓ Nerve growth factor

Oligodendrocyte
↑ Oligodendrogliosis

Myelin
↑ Abnormal myelination

Synapse
↓ Neurotransmitter
↓ Synaptic plasticity

Microglia
↑ Microglial activation
↑ Chronic inflammation

Astrocyte
↑ Astrogliosis

b Functional changes during normal aging

Cognitive decline
• Vocabulary
• Conceptual reasoning
• Memory
• Processing speed

Mental deficits
• Anxiety
• Depression

Sleep disruption
• Poor sleep quality
• Delayed sleep onset latency

Circadian dysfunction
Disruption of amplitude and period length of circadian behaviour

Appendix 3. Normal brain ageing drives the progressive impairment of cognitive, social and physical abilities through various aspects (taken from Satoh et al., 2017).
a Throughout the aging process, the formation of amyloid plaques and neurofibrillary tangles occurs both inside and outside neurons. Adult neurogenesis declines, along with a reduction in nerve growth factor concentration, while persistent chronic low-grade inflammation results from microglial activation. Additionally, there is a significant age-related decrease in neurotransmitter production and synaptic plasticity. The proper myelination of CNS neurons may also face disruption, accompanied by an increase in brain oligodendrogliosis and astrogliosis. **b** Changes in brain function associated with

61

aging encompass cognitive and mental deficits, sleep disturbances, and circadian dysfunction. Cognitive functions affected by age include vocabulary, conceptual reasoning, memory, and processing speed. Mental health concerns, such as anxiety or depression, and sleep disruptions, like poor sleep quality or delayed sleep onset latency, are notably heightened in the elderly. Ultimately, age-associated circadian dysfunction is implicated in disrupting the amplitude and period length of circadian behaviors.
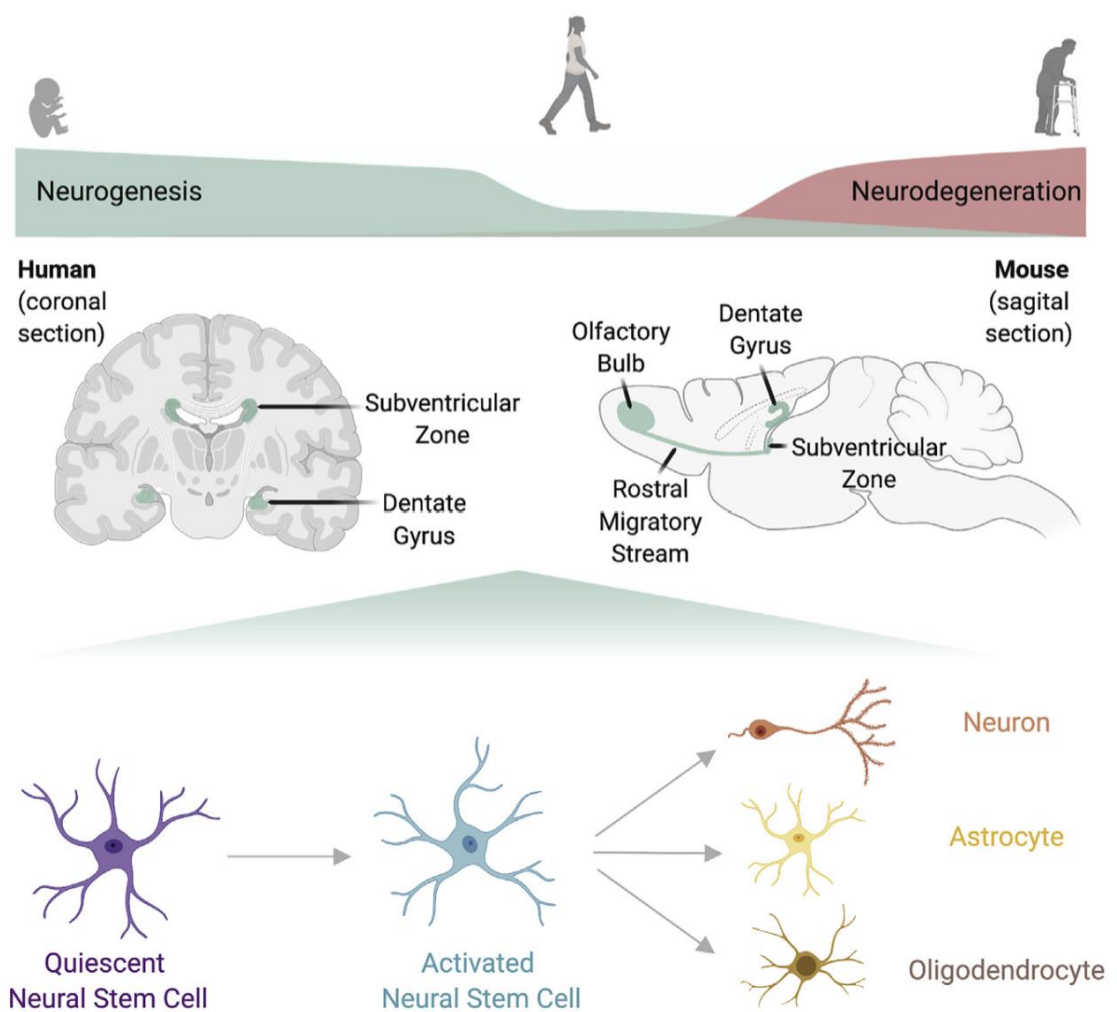
Appendix 4. Adult neurogenesis declines with age (taken from Negredo et al., 2020).
The capacity of NSCs to proliferate and generate new neurons experiences a marked decline post-development, persisting throughout the aging process. Concurrently, there is an escalation in the occurrence of neurodegeneration and age-related diseases, as

illustrated in the conceptual trajectories for neurogenesis and neurodegeneration in the diagram. The adult mammalian brain harbors two reservoirs of regenerative NSCs: the DG of the hippocampus and the SVZ of the lateral ventricles (depicted in teal green). Within these niches, qNSCs can be activated to give rise to aNSCs. aNSCs possess the potential to differentiate into neurons, oligodendrocytes, or astrocytes.
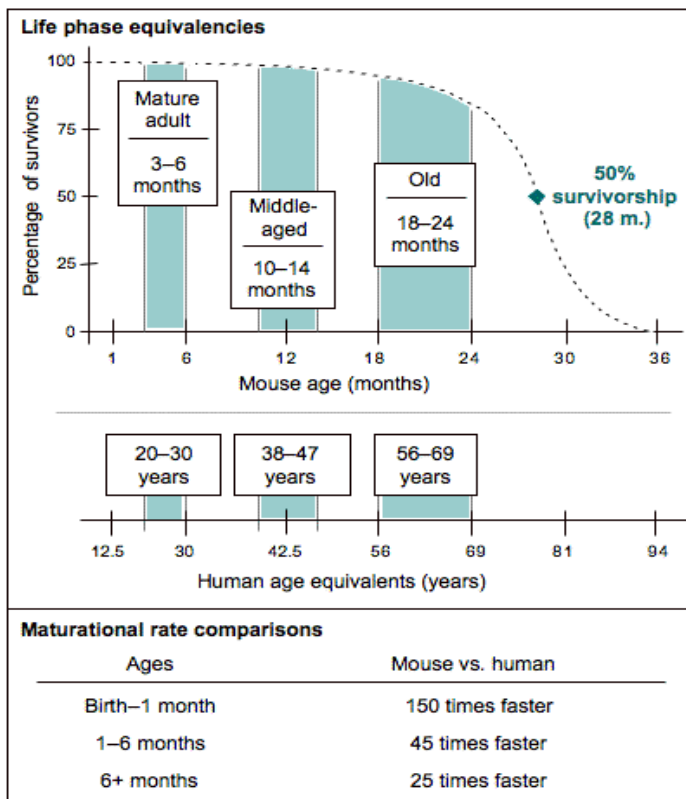
Appendix 5. The age of the mice is selected according to the corresponding age of the human (taken from Kevin Flurkey, 2007).

Mature life history stages in C57BL/6J mice, in comparison to human beings, are represented by the following age ranges: Mature adult (3–6 months of age), Middle age (10–15 months of age), and Old (18–24 months of age or older, depending on genotype).